



Sigma-1 Receptors Control Neuropathic Pain and Peripheral Neuroinflammation After Nerve Injury in Female Mice: A Transcriptomic Study

M. Carmen Ruiz-Cantero^{1,2,3} · José M. Entrena^{2,3,8} · Antonia Artacho-Cordón^{1,2,3} · Miguel Á. Huerta^{1,2,3} · Enrique Portillo-Salido⁴ · Francisco R. Nieto^{1,2,3} · José M. Baeyens^{1,2,3} · Michael Costigan^{5,6} · Rafael González-Cano^{1,2,3} · Enrique J. Cobos^{1,2,3,7}

Received: 20 December 2023 / Accepted: 5 August 2024

© The Author(s), under exclusive licence to Springer Science+Business Media, LLC, part of Springer Nature 2024

Abstract

The mechanisms for neuropathic pain amelioration by sigma-1 receptor inhibition are not fully understood. We studied genome-wide transcriptomic changes (RNAseq) in the dorsal root ganglia (DRG) from wild-type and sigma-1 receptor knockout mice prior to and following Spared Nerve Injury (SNI). In wildtype mice, most of the transcriptomic changes following SNI are related to the immune function or neurotransmission. Immune function transcripts contain cytokines and markers for immune cells, including macrophages/monocytes and CD4+T cells. Many of these immune transcripts were attenuated by sigma-1 knockout in response to SNI. Consistent with this we found, using flow cytometry, that sigma-1 knockout mice showed a reduction in macrophage/monocyte recruitment as well as an absence of CD4+T cell recruitment in the DRG after nerve injury. Sigma-1 knockout mice showed a reduction of neuropathic (mechanical and cold) allodynia and spontaneous pain-like responses (licking of the injured paw) which accompany the decreased peripheral neuroinflammatory response after nerve injury. Treatment with maraviroc (a CCR5 antagonist which preferentially inhibits CD4+T cells in the periphery) of neuropathic wild-type mice only partially replicated the sigma-1 knockout phenotype, as it did not alter cold allodynia but attenuated spontaneous pain-like responses and mechanical hypersensitivity. Therefore, modulation of peripheral CD4+T cell activity might contribute to the amelioration of spontaneous pain and neuropathic tactile allodynia seen in the sigma-1 receptor knockout mice, but not to the effect on cold allodynia. We conclude that sigma-1 receptor inhibition decreases DRG neuroinflammation which might partially explain its anti-neuropathic effect.

Keywords Sigma-1 receptor · Neuropathic pain · Neuroinflammation · T cell · Macrophage · Artificial intelligence

✉ Rafael González-Cano
rgcano@ugr.es

✉ Enrique J. Cobos
ejcobos@ugr.es

¹ Department of Pharmacology, Faculty of Medicine, University of Granada, Granada 18016, Spain

² Institute of Neuroscience, Biomedical Research Center, University of Granada, Armilla, Granada 18100, Spain

³ Biosanitary Research Institute ibs.GRANADA, Granada 18012, Spain

⁴ Faculty of Health Sciences, International University of La Rioja (UNIR), Logroño, La Rioja 26004, Spain

⁵ Department of Neurobiology, Harvard Medical School, Boston, MA 02115, USA

⁶ Department of Anaesthesia, Boston Children's Hospital, Boston, MA 02115, USA

⁷ Teófilo Hernando Institute for Drug Discovery, Madrid 28029, Spain

⁸ Animal Behavior Research Unit, Scientific Instrumentation Center, Parque Tecnológico de Ciencias de la Salud, University of Granada, Armilla, Granada 18100, Spain

Introduction

Sigma-1 receptor is a Ca^{2+} -sensing chaperone with an important modulatory role in pain neurotransmission. Specifically, sigma-1 receptors are considered a promising target for the treatment of neuropathic pain (Merlos et al. 2017; Ruiz-Cantero et al. 2021). The anti-neuropathic effect of sigma-1 receptor inhibition is classically attributed to a decrease in sensory amplification within the spinal cord (central sensitization) (reviewed by Merlos et al. 2017). However, we recently reported that sigma-1 receptors can also prominently modulate the sensitization of peripheral nociceptive neurons (Ruiz-Cantero et al. 2023a, b). Indeed, sigma-1 receptors are known to be expressed at much higher levels in the dorsal root ganglion (DRG), where the somas of peripheral sensory neurons are located, than in the spinal cord dorsal horn (Sánchez-Fernández et al. 2014). It is worth noting that all DRG neurons express sigma-1 receptors in mice (Montilla-García et al. 2018; Bravo-Caparrós et al. 2020), rats (Shin et al. 2022) or humans (Ruiz-Cantero et al. 2023b).

The pivotal contribution of immune and glial cells to the development and maintenance of neuropathic pain has been firmly established in recent decades (Ji et al. 2014, 2018; Ruiz-Cantero et al. 2021; Ghazisaeidi et al. 2023). However, the modulation of neuroinflammation by sigma-1 receptors during nerve injury has only been sparsely explored. Studies show that sigma-1 receptor antagonism decreases astrogliosis in the dorsal spinal cord of animals with peripheral neuropathic pain (Moon et al. 2014, 2015). In addition, a decrease in spinal microgliosis by sigma-1 receptor inhibition after peripheral nerve injury was recently found (Denaro et al. 2023). To date, only one study explored the role of sigma-1 receptors on peripheral neuroinflammation during chronic pain, demonstrating that sigma-1 receptor knockout (KO) mice exhibited decreased macrophage/monocyte infiltration into the DRG after nerve injury in comparison to wild-type (WT) mice (Bravo-Caparrós et al. 2020). In addition to macrophages, other immune cells participate in peripheral neuropathic neuroinflammation such as T cells (Cobos et al. 2018). However, there are no studies exploring the possible modulatory role of sigma-1 receptors on these mechanisms.

The SNI (Spared Nerve Injury) model consists of the transection of the tibial and common peroneal branches of the sciatic nerve, and it is known to induce hundreds of transcriptional changes in the DRG, including transcripts corresponding to the peripheral neuroinflammatory process (Costigan et al. 2010; Cobos et al. 2018). With the aim to obtain a comprehensive analysis of the effect of sigma-1 deletion in the processes that occur at peripheral level after nerve injury, we studied genome-wide transcriptomic

changes (by RNAseq) after SNI injury in the DRG in WT and sigma-1 receptor KO mice. The SNI is known to induce not only sensory hypersensitivity to several stimuli (Cobos et al. 2018; Bravo-Caparrós et al. 2020), but also spontaneous pain-like behaviors (Zheng et al. 2022). This is important since spontaneous pain is thought to have much stronger clinical repercussions than cutaneous sensitivity (Mogil et al. 2010; Zheng et al. 2022). Sigma-1 receptor KO mice are well known to show a decreased neuropathic sensory hypersensitivity (de la Puente et al. 2009; Bravo-Caparrós et al. 2019, 2020), although whether they have reduced spontaneous pain has not been explored. Therefore, we also aimed to delve deeper into the phenotype of sigma-1 receptor knockout mice to explore not only standard hypersensitivity to sensory stimuli but also possible alterations in spontaneous pain-like behaviors.

Methods

Experimental Animals

Experiments were performed in wild-type (WT) CD-1 mice (Charles River, Barcelona, Spain) and in sigma-1 receptor knockout (KO) mice (Animal Experimentation Unit - CIC UGR, Granada, Spain), weighing 25–30 g (8 to 11 weeks old). Women show a higher prevalence of pain than men in most chronic neuropathic pain conditions. However, pre-clinical studies have clearly been dominated by the use of male animals, and only in recent years female animals have been frequently incorporated into basic research (reviewed by Ghazisaeidi et al. 2023). In this study we used female animals in all experiments. Knockout mice were generated on a CD-1 background as previously described (Entrena et al. 2009), by using a traditional backcrossing breeding strategy with WT progenitors from Charles River for at least 15 generations, which theoretically ensured that the genetic material from the original background is virtually absent (Wong 2002). Animals were housed in colony cages (10 mice per cage), in a temperature-controlled room (22 ± 2 °C) with an automatic 12-h light/dark cycle (08:00–20:00 h). An igloo and a plastic tunnel were placed in each housing cage for environmental enrichment. Animals were fed a standard laboratory diet and tap water ad libitum until the beginning of the experiments. The behavioral experiments were performed during the light phase (from 9:00 a.m. to 3:00 p.m.). The mice were randomized to treatment groups, testing each day a balanced number of animals from several experimental groups, and they were also tested randomly throughout the estrous cycle. Mice were handled in accordance with international standards (European Communities Council directive 2010/63), and the experimental protocols were

approved by regional (Junta de Andalucía) and Institutional (Research Ethics Committee of the University of Granada) authorities. To decrease the number of animals in this study, we used the same mice for behavioral studies and immunostaining or fluorescence-activated cell sorting (FACS), when possible.

Spared Nerve Injury

The spared nerve injury (SNI) was performed as previously described (Decosterd and Woolf 2000). Briefly, an incision was made in the left thigh skin and through the biceps femoris muscle, at the site of trifurcation of the sciatic nerve, and its three terminal branches (the sural, common peroneal, and tibial nerves) were exposed. The tibial and common peroneal branches were ligated with a silk suture and transected distally, while the sural nerve was left intact. In sham-operated control mice, the sciatic nerve terminal branches were exposed but not ligated. Mice were anesthetized with 4% isoflurane (IsoVet[®], B. Braun, Barcelona, Spain) in oxygen. During the surgical procedure, anesthesia was maintained with 2.5% isoflurane delivered via a nose cone. Wounds were closed and the animals returned to their cages. We monitor carefully for signs of distress after surgery. Although mice can move, rise, and get access to food and water normally after surgery, we place some food pellets on the cage floor to facilitate access to them. Autotomy behavior was not observed in any animal following SNI during this study. Sample collections and behavioral assays were made 7 days after surgery, as it is known that sensory hypersensitivity and DRG neuroinflammation has fully developed 7 days post SNI (e.g. Cobos et al. 2018; Bravo-Caparrós et al. 2019, 2020).

RNA Analysis

RNA Preparation

The lumbar L3 and L4 dorsal root ganglia (DRGs) were carefully removed from naïve WT and sigma-1 receptor KO mice, and from mice from both genotypes 7 days after SNI surgery. We selected L3 and L4 DRGs because they contain all somas from the common peroneal and tibial branches of the sciatic nerve (Laedermann et al. 2014) which are injured during SNI (see 2.2 for details). We studied DRGs collected in five biological replicates in samples from naïve WT or sigma-1 receptor KO mice, and in four biological replicates from mice with SNI. Each biological replicate was obtained from six mice (twelve ipsilateral L3/4 DRGs or six ipsilateral dSCs). Samples were immediately frozen after dissection in 2 ml eppendorf tubes in contact with dry ice and stored at -80°C until use. RNA was extracted using

the RNeasy Plus Universal Min Kit (QIACube / QIAGEN) according to the manufacturer's instructions. Concentration and quality of extracted RNA were measured using the Qubit 4 Fluorometer (Thermo Fisher Scientific, MA, USA) and the 2100 Bioanalyzer Instrument (Agilent Technologies, CA, USA). Sample processing was carried out in the genomics unit of the Pfizer-University of Granada-Junta de Andalucía Center for Genomics and Oncological Research (GENYO).

Next-Generation Transcriptome Sequencing (RNA-Seq) for Gene Expression Analysis

Libraries from mRNA were prepared using 1 µg of RNA starting material and the TruSeq Stranded mRNA Library Prep Kit (Illumina, CA, USA) according to the manufacturer's protocol. This protocol captures poly-adenylated RNA by transcription by oligo-dT primer, after which the RNA is fragmented. The sample was back transcribed to generate the cDNA, both in the first and second strands. The 3' ends were adenylated, the adapters and barcodes were ligated, and finally, it was enriched by PCR. Adapters and samples codes (index-barcodes) were added to the libraries to be able to be sequenced simultaneously. mRNA libraries were sequenced on the NextSeq 500 system (Illumina, CA, USA) using the highest output mode and paired-end 75 bp read lengths with a depth of 25–30 million reads for each sample. Sequencing was performed in the genomics unit of GENYO.

Expression data can be found in Gene Expression Omnibus (GEO) database, with accession number GSE241361.

Bioinformatics

FastQS were obtained using Illumina's bcl2fastq software. The quality of the sequences was screened using fastQC, qualimap (Okonechnikov et al. 2016) and multiQC (Ewels et al. 2016). Using the RSEM pipeline (Li and Dewey 2011), the gene expression was obtained by mapping RNAseq reads with hisat2 aligner (Kim et al. 2019) to the Gencode mouse genome GRCm38 and annotated with the vM25 gtf (Frankish et al. 2021). The differential expression was normalised with NOISeq (Tarazona et al. 2011) following the approach of Trimmed Mean of M values (Gu et al. 2016). The differential expression analysis was performed with the default recommendations of DESeq2 (Love et al. 2014). Transcripts were considered significantly regulated when the *P* value < 0.01. A threshold fold change of 1.4 was imposed for each transcript to be included in the analysis, similar than in previous transcriptomic studies (Costigan et al. 2010; Yokoyama et al. 2020). To better analyze the differences in WT vs. sigma-1 receptor KO mice during the naïve

condition and after SNI, we constructed a Weighted Gene Co-expression Network Analysis (WGCNA) using the regulated transcripts in the 4 groups of samples (naïve WT vs. naïve KO and SNI WT vs. SNI KO) to find groups of genes (modules) with similar expression changes across the experimental conditions tested. Briefly, we computed the absolute Pearson correlation coefficients between each transcript and every other transcript in the expression dataset; these values were used to determine the topological overlap, a measure of connection strength, or ‘neighborhood sharing’, in the network. This results in modules of co-expressed genes where the members of each network have high topological overlap in their patterns of regulation (Horvath et al. 2006; Cobos et al. 2018). WGCNA and the similarity plot of the module eigengenes from each module were done with its corresponding R’s package (Langfelder and Horvath 2008), considering an unsigned network for the topological overlap matrix calculated with a bidweight midcorrelation.

Heat maps were generated using HeatMapImage tool from GenePattern software (v. 3.9.11). To facilitate comparison of transcriptional regulation in the different experimental conditions, the height of heat maps shown maintained the same proportion with the number of regulated transcripts throughout all figures.

To identify the functional categories most prominently represented in the lists of regulated transcripts and in the modules obtained using the WGCNA we made functional Enrichment Analyses analyzing gene lists with Ingenuity Pathway Analysis (IPA) software, version 84,978,992 (Qiagen, USA). This program can identify the annotations for each gene of a given set in its database, which is constructed from previously published information, and calculates the most over-represented descriptors in the list to return a Benjamini-Hochberg (B-H) adjusted *P* value as a measure of the enrichment in each functional subdivision.

CFA-Induced Peripheral Inflammation

To compare the immune cell recruitment due to paw inflammation in WT and sigma-1 receptor KO mice, 10–20 μ L of complete Freund’s adjuvant (CFA; Sigma-Aldrich) was injected into the right hindpaw of mice from each genotype, using a 1710 TLL Hamilton microsyringe (Hamilton Company, NV, USA) with a 30½-gauge needle. Seven days after the injection, the paws were dissected and the immune cell recruitment was measured by FACS. As a control of the immune cell presence in noninflamed tissue, we used samples from the paw contralateral to the injection, as well as samples from naïve mice and from mice injected with 20 μ L of saline.

Fluorescence-Activated Cell Sorting (FACS)

FACS was used to determine the immune cell populations in wild type and sigma-1 receptor KO mice after SNI. Each sample contained the ipsilateral L3 and L4 DRGs from six animals with SNI. The DRGs contralateral to the nerve injury were used as a control. As an additional control, we also tested both left and right L3 and L4 DRGs from 3 naïve animals (12 DRGs in all cases). To study immune cell recruitment after paw inflammation in mice from both genotypes, we tested plantar tissue from animals injected with CFA, using tissue from the paw contralateral to the injection as a control, as well as paw tissue from naïve mice. In all cases, mice were euthanized by cervical dislocation and DRGs or plantar tissue were dissected and digested with collagenase IV (1 mg/mL, LS004188, Worthington, Lakewood, NJ, USA) and DNase I (0.1%, LS002007, Worthington) for 1 h at 37 °C with agitation. The digestion was neutralized washing with PBS. Cells of DRGs were gently pipetted up and down, in a PBS with DNase I solution, to obtain a single cell suspension. In case of plantar tissue, samples were mechanically crushed over a 70 μ m filter. Then samples were filtered in a tube with cell strainer cap (pore size 35 μ m) and the rat anti-CD32/16 antibody (1:100, 20 min, 553141; Biolegend, San Diego, CA) was used to block Fc- γ RII (CD32) and Fc- γ RIII (CD16) binding to IgG. Cells were incubated with antibodies recognizing the hematopoietic cell marker CD45 (1:200, 103108, clone 30-F11, Biolegend), the myeloid marker CD11b (1:100, 101227, clone M1/70, Biolegend), the neutrophil-specific marker Ly6G (1:100, 127617, clone 1A8, Biolegend), the B cells CD45R/B220 (1:200, 103239, clone RA3-6B2, Biolegend), the T cells marker TCR β (1:100, 553174, clone H57-597, BD Biosciences, San Jose, CA, USA), the CD4 marker (1:160, 100555, clone RM4-5, Biolegend) and the CD8a marker (1:80, 100752, clone 53–6.7, Biolegend), together with a viability dye (1:1000, 65-0865-14, Thermo Fisher Scientific), for 30 min on ice. The populations of macrophages/monocytes (CD45 + CD11b + Ly6G – cells), neutrophils (CD45 + CD11b + Ly6G + cells), B cells (CD45 + CD45R/B220+), T cells (CD45 + TCR β +), CD4 T cells (CD45 + TCR β + CD4+) and CD8 T cells (CD45 + TCR β + CD8a+) were determined from the markers indicated above in cells labeled with the viability dye. Before and after incubation with the antibodies, the cells were washed three times in 2% FBS/PBS (FACS buffer). Cells were fixed with paraformaldehyde (2%, 158127, Sigma-Aldrich) for 20 min, and on the next day samples were assayed with a BD FACSymphony A5 flow cytometer (BD Biosciences). Compensation beads were used as compensation controls, and fluorescence minus one (FMO) controls were included to determine the level of nonspecific

staining and autofluorescence associated with different cell subsets. All data were analyzed with FlowJo 2.0 software (Treestar, Ashland, OR, USA).

Immunohistochemistry

On day 7 after surgery, SNI mice were anesthetized with 4% isoflurane (in oxygen) and perfused transcardially with 0.9% saline solution followed by 4% paraformaldehyde (Sigma-Aldrich). The lumbar L4 DRG, were injured and noninjured neurons coexist (Laedermann et al. 2014), were dissected and post-fixed for 1 h in the same paraformaldehyde solution. Embedding procedure differed depending on the staining to be performed, as not all antibodies used showed optimal results in all embedding media. Samples for sigma-1 receptor immunostaining were dehydrated and embedded in paraffin. Tissue Sect. 5 µm thick were cut with a sliding microtome, mounted on microscope slides (Sigma-Aldrich), deparaffinized in xylol (Panreac Quimica, Castellar del Valls, Spain) and rehydrated before antigen retrieval (steam heating for 22 min with 1% citrate buffer, pH 8). Samples for the staining of immune cells were incubated for 48 h in 30% sucrose (Sigma-Aldrich) at 4°C to be embedded in O.C.T Tissue-Tek medium (Sakura Finetek, Barcelona, Spain), and frozen and stored at -80° C until their immunohistochemical study. Sections of 15 µm thick were cut with a cryostat and thaw-mounted onto Superfrost Plus microscope slides (Thermo Fisher Scientific).

Tissue sections were incubated for 1 h in blocking solution with 5% normal goat serum, 0.3% Triton X-100, and 0.1% Tween 20 in Tris buffer solution. Then, the slides were incubated with the primary antibodies in blocking solution. The primary antibodies used for the immunostaining of neurons in combination with the sigma-1 labelling were: mouse anti-sigma-1 receptor (1:200, sc-137075, Santa Cruz Biotechnology, Inc, Heidelberg, Germany) and rabbit anti-NeuN (neuronal nuclei) (1:500, ABN78, Merck Millipore, MA, USA). The primary antibodies for the immunostaining of neurons in combination with immune cells were: mouse anti-NeuN conjugated with Alexa Fluor 555 (1:500, MAB377A5) for the neuronal staining, and the antibodies labelling immune cell populations: rabbit anti-Allograft Inflammatory Factor 1 (AIF1, 1:1000, 019-19741, Wako Chemical, Neuss, Germany), also known as ionized calcium-binding adapter molecule 1 (IBA-1), and rat anti-mouse CD3 (1:200, 555273, BD Biosciences).

Incubation with the primary antibody for sigma-1 receptor lasted for 1 h at room temperature (RT), whereas incubation with the anti-AIF1 and the anti-CD3 antibodies lasted overnight at 4 °C. After incubation with the primary antibodies, sections were washed three times for 10 min and incubated with the appropriate secondary antibodies for 1 h

at RT. The secondary antibodies used were Alexa Fluor-488 goat anti-mouse (1:500, A-11029, Thermo Fisher Scientific) and Alexa Fluor-594 goat anti-rabbit (1:500, A-11012, Thermo Fisher Scientific), in the experiments labelling sigma-1 receptor and NeuN, and Alexa Fluor-647 goat anti-rabbit (1:500, A-21245, Thermo Fisher Scientific) and Alexa Fluor-488 goat anti-rat (1:500, A-11006, Thermo Fisher Scientific) in the experiments for the labelling of immune cells. In this latter case, after incubation with the secondary antibodies, sections were washed again three times for 10 min and incubated with the conjugated anti-NeuN antibody also for 1 h at RT.

Finally, slides were washed three times for 10 min before the mounting procedure and they were coverslipped with ProLong Gold Antifade mounting medium (Thermo Fisher Scientific). Images were acquired with a confocal laser-scanning microscope (Model ZEISS LSM 900, Carl Zeiss Microscopy, NY, USA).

Maraviroc Administration

The day before the SNI, a baseline measurement of the von Frey threshold and the responses to the cold stimulus (acetone) were recorded. Then, the CCR5 antagonist maraviroc was orally administered until day 7 after surgery, when the sensory evaluation took place. Mice were fed with the same diet as the control group, but received 300 mg/L maraviroc (Sigma-Aldrich, Madrid, Spain) in the drinking water. The dose of maraviroc was selected based on previous studies (Ochoa-Callejero et al. 2013; Pérez-Martínez et al. 2020). This drug concentration in the drinking water results in an approximate daily dose of 50 mg/kg for a mouse of 30 g weight and a daily intake of 5 ml of drinking water, which is the average water consumption under the housing conditions of our mice. The drinking water with the diluted drug was prepared and poured into a 100 ml drinker, which was changed every day to avoid possible degradation of the drug. Control mice received drinking water without any additives.

Assessment of Mechanical Allodynia

Mechanical thresholds were tested before surgery (baseline) and 7 days after SNI. Mechanical allodynia was assessed with von Frey filaments according to a previously described method, with slight modifications (Bravo-Caparrós et al. 2020). On each day of evaluation the mice were habituated for 60 min in individual transparent plastic chambers (7 × 7 × 13 cm) with a floor made of wire mesh. After the acclimation period, calibrated von Frey monofilaments (Stoelting, Wood Dale, IL, USA) with bending forces that ranged from 0.02 to 1.4 g were applied with the up-down paradigm in the sural nerve

territory, starting with the 0.6 g filament, and allowing 10 s between successive applications. The response to the filament was considered positive if immediate flinching, licking/biting or rapid withdrawal of the stimulated paw was observed. In each consecutive test, if there was a positive response, a weaker filament was then used; if there was no response to the filament, a stronger stimulus was then selected. This sequence was repeated 4 times to limit the values of the mechanical threshold. Behavioral evaluations were performed by an observer blinded to the mouse genotype or pharmacological treatment.

Assessment of Cold Allodynia

Cold sensitivity was tested before surgery (baseline) and 7 days after SNI. Cold allodynia was tested by gently touching the plantar skin of the hind paw with an acetone drop, as previously described (Cobos et al. 2018). On each day of evaluation the mice were housed and habituated for 30 min in individual transparent plastic enclosures (7×7×13 cm) with a floor made of wire mesh. Acetone was applied three times to the ipsilateral hind paw at intervals of 30 s, and the duration of biting or licking of the hind paw was recorded with a stopwatch and reported as the cumulative time of biting/licking in all three measurements. A cutoff time of 10 s was used in each of the three trials, because animals rarely licked their hind paw for more than 10 s. During the pre-surgery baseline evaluation we discarded ≈5% of the mice tested due to an exaggerated atypical response to the acetone (> 2 s of cumulative responses to acetone in the three measures).

Evaluation of Spontaneous Pain-Like Behaviors

To evaluate spontaneous pain-like behaviors we built in house a device to record the mice in their home cage, and performed an in-depth video analysis using an algorithm suitable for analyzing the behaviors of the mice, as it is described below.

Video Setup and Recording

To monitor the behavior of the animals, we constructed a recording system, which consisted of a methacrylate structure holding a high-resolution infrared video camera (1440×1024 pixels) (Kuman RPi Camera, USA). This structure was placed above the home cage, which was a standard transparent methacrylate cage (16 wide x 22 cm long x 14 cm high). Each camera was equipped with two infrared light-emitting diodes (IR-LEDs) to minimize the influence of ambient light on the recordings. The camera was controlled by a Raspberry Pi Zero single-board

computer (Kubii, France) that stored the video recordings on USB sticks, which can be later transferred to a computer for subsequent analysis. The recordings were captured at a rate of 10 frames per second. Naïve animals, or animals after SNI or sham surgery, were single-housed in the recording devices with food and water ad libitum, starting 7 days after the procedure, and during a maximum of 72 h (from Friday at 10:00 AM till Monday at 9:00 AM). Only the data of the last 48 h was considered for analysis. We built 8 devices to simultaneously record 8 animals. A picture of the device is shown in Fig. S1A.

Video Analysis and Clustering of Behaviors

We used DeepLabCut™ software to automatically label the positions of specific body parts of the animals (nose, right ear, left ear, neck, back, right thigh, left thigh, base of the tail) in each frame of the recordings. The labeled body parts of the mice are depicted in Fig. S1B. The automatic detection of those key anatomical features of each animal makes possible to calculate their relative coordinates and hence the postures of the animals. In addition, it is also possible to objectively quantify the differences in the position of these body parts between frames to measure the displacement of the labels (e.g. the movement of the animal or a body part). The data were grouped into one-second intervals (i.e., 10 consecutive frames) and compressed using a variational autoencoder (VAME) (Fig. S1C).

We then applied the K-Means algorithm to cluster the data from naïve and SNI mice into distinct behavioral groups in an unsupervised manner. We initially fit K-Means to 100 groups and then eliminated the clusters that exhibited a frequency below 1%. From all behaviors recorded, we specifically selected asymmetrically directed clusters of behaviors that involved the approach of the head of the animal to the injured limb for quantification and further analysis. These clusters will be defined as pain-like behaviors and include for instance licking or biting the injured limb. The clusters that implied a sustained approach of the head to the limb (e.g. some postures where the mouse is sleeping), were not considered for the analysis. Once the clusters of pain-like responses were selected, they were used for quantification. As we found statistically significant differences in the time spent performing these pain-like responses between naïve and SNI mice (as it will be described in the Sect. 3.6), we used the previously trained K-Means to look for this specific group of behaviors in new recordings from all other experimental groups (e.g. the behavior of uninjured and SNI sigma-1 KO mice, or the behavior of neuropathic mice after treatment with maraviroc or its control). All

scripts employed in the analysis were written in Python (version 3.5). The computational processing was performed on a computer equipped with an Intel® Core™ i9-9820X CPU @ 3.30 GHz and an NVIDIA 2080Ti graphics processing unit (GPU), providing significant computational power for the video analysis and machine learning tasks.

Data Analysis of the Expression of Individual Genes, Behavioral and FACS Experiments

The data were analyzed with the SigmaPlot 12.0 program (Systat Software Inc., San Jose, CA, USA). For the statistical analysis of the expression of individual genes, we used a two-way analysis of variance (ANOVA). For behavioral studies, statistical analysis was carried out with two-way repeated-measures ANOVA. For the results from FACS assays statistical analysis was performed with two-way ANOVA. The Student-Newman-Keuls post-test was used in all cases. The differences between means were considered significant when the *P* value was below 0.05.

Results and Discussion

Transcriptional Profile of the DRG from Naïve Sigma-1 Receptor KO Mice

We evaluated global gene expression of the L3/L4 DRGs from naïve WT and naïve sigma-1 receptor KO mice by RNAseq. A heat map of the differentially expressed transcripts, where the intensity of the color represents changes in gene expression (not absolute values), is shown in Fig. 1A. We found significant differences in the expression of 1156 transcripts between genotypes, with 547 of them upregulated in the sigma-1 receptor KO mice (light blue in WT; dark blue in KO) and 609 transcripts downregulated in the sigma-1 receptor KO mice (dark blue in WT; light blue in mutant mice, Fig. 1A). The genes whose expression significantly differ in the DRG from uninjured mice from both genotypes (WT and sigma-1 receptor KO) are identified in Table S1.

Next, we performed a functional enrichment analysis of the DRG transcripts that show differential expression between genotypes. Transcripts expressed at higher levels in the KO DRGs demonstrate a significant enrichment

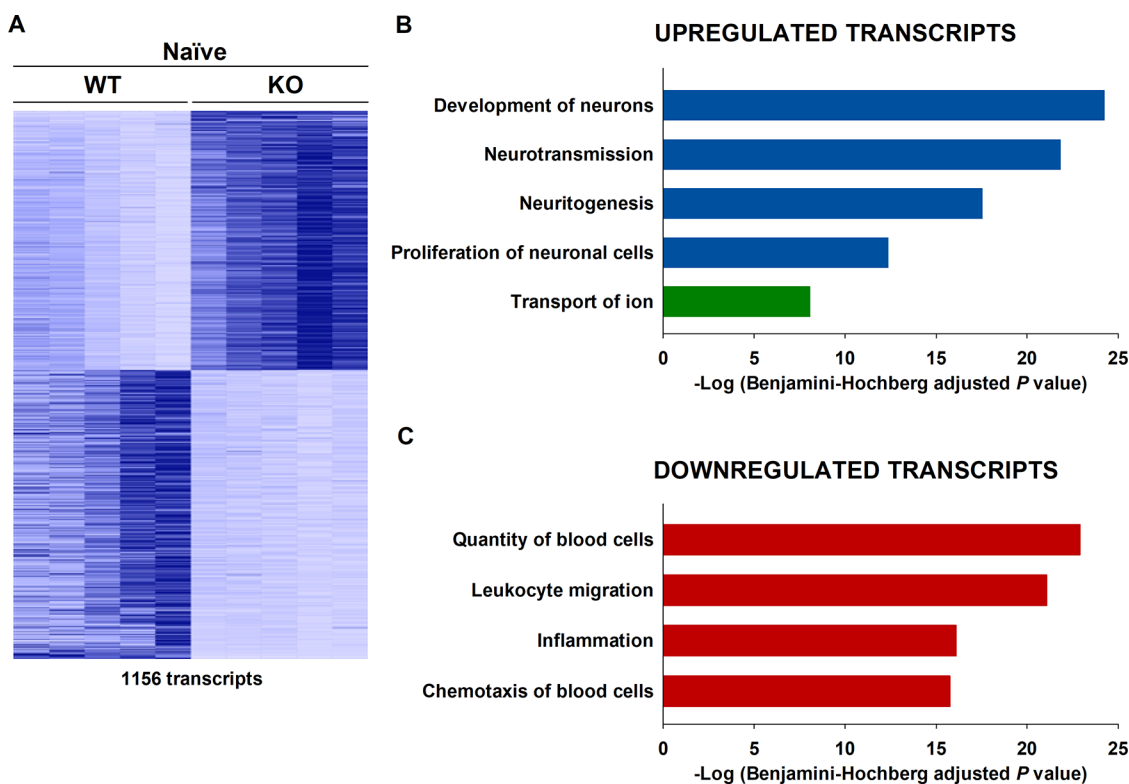


Fig. 1 Comparison of the transcriptional profile of the dorsal root ganglia (DRG) from naïve wild-type (WT) and sigma-1 receptor knockout (KO) mice. **(A)** Heatmap of the relative expression of the transcripts from the L3-L4 DRG with significant differences ($P < 0.01$) and a fold change of at least 1.4) between naïve WT and KO mice. Light blue represents low-level expression and dark blue high-level expression.

The total number of regulated transcripts is indicated. **(B-C)** Representative functional characteristics sorted by the strength of statistical significance ($-\log$ of Benjamini-Hochberg adjusted *P*-value) that IPA software ascribed the function given, using the lists of transcripts **(B)** upregulated or **(C)** downregulated by the knockout of sigma-1 receptor gene

for the annotation of neuronal functions, which include functions such as “Development of neurons”, “Neurotransmission”, “Neuritogenesis”, or “Proliferation of neuronal cells”, with B-H P values ranging from 10^{-13} to 10^{-25} . “Transport of ion”, which is enriched in neuronal ion channels, was also present with a B-H P value of 10^{-8} (Fig. 1B). The description of the content of the functional annotations for the KO enriched transcripts is shown in Table S2.

We and others have previously reported by immunohistochemical experiments that within the DRG, sigma-1 receptors are exclusively present in sensory neurons (Montilla-García et al. 2018; Bravo-Caparrós et al. 2020; Shin et al. 2022; Ruiz-Cantero et al. 2023b). Therefore, the alterations in neuronal genes could be explained as a direct consequence of the absence of sigma-1 receptors in these cells. Despite the large number of neuronal genes with increased expression in the naïve KO DRG, these mutant mice do not have any overt basal sensory phenotype relative to WT, as shown in numerous previous studies (reviewed in Tsai et al. 2009; Merlos et al. 2017; Ruiz-Cantero et al. 2021). However, under conditions which normally induce a sensitization of the nociceptive system, such as after administration of chemical algogens or in pathological pain models, sigma-1 receptor KO mice show a decreased sensitization (reviewed Tsai et al. 2009; Merlos et al. 2017; Ruiz-Cantero et al. 2021). Therefore, basal transcriptional alterations in neuronal genes shown here in sigma-1 receptor KO mice might reflect a state which dampens nociceptive sensitization.

The analysis of the transcripts which were downregulated in the KO mice relative to WT yielded starkly divergent results, since all functional annotations retrieved were related with the actions and functioning of the immune system, such as “Quantity of blood cells”, “Leukocyte migration”, “Inflammation” or “Chemotaxis of blood cells”, with B-H P value ranging from 10^{-16} to 10^{-23} (Fig. 1C). The description of the content of the functional annotations of the downregulated transcripts is shown in Table S3. It is known that neurons are the major source of some chemokines in the DRG, such as CCL2 (Zhu et al. 2014) and here we show that naïve sigma-1 receptor KO mice have a decreased expression in several chemokines, including CCL2. It could be hypothesized that the absence of sigma-1 receptors in sensory neurons could alter the production of neuronal-derived chemokines, which in turn might have an impact on the baseline recruitment/activation of resident immune cells.

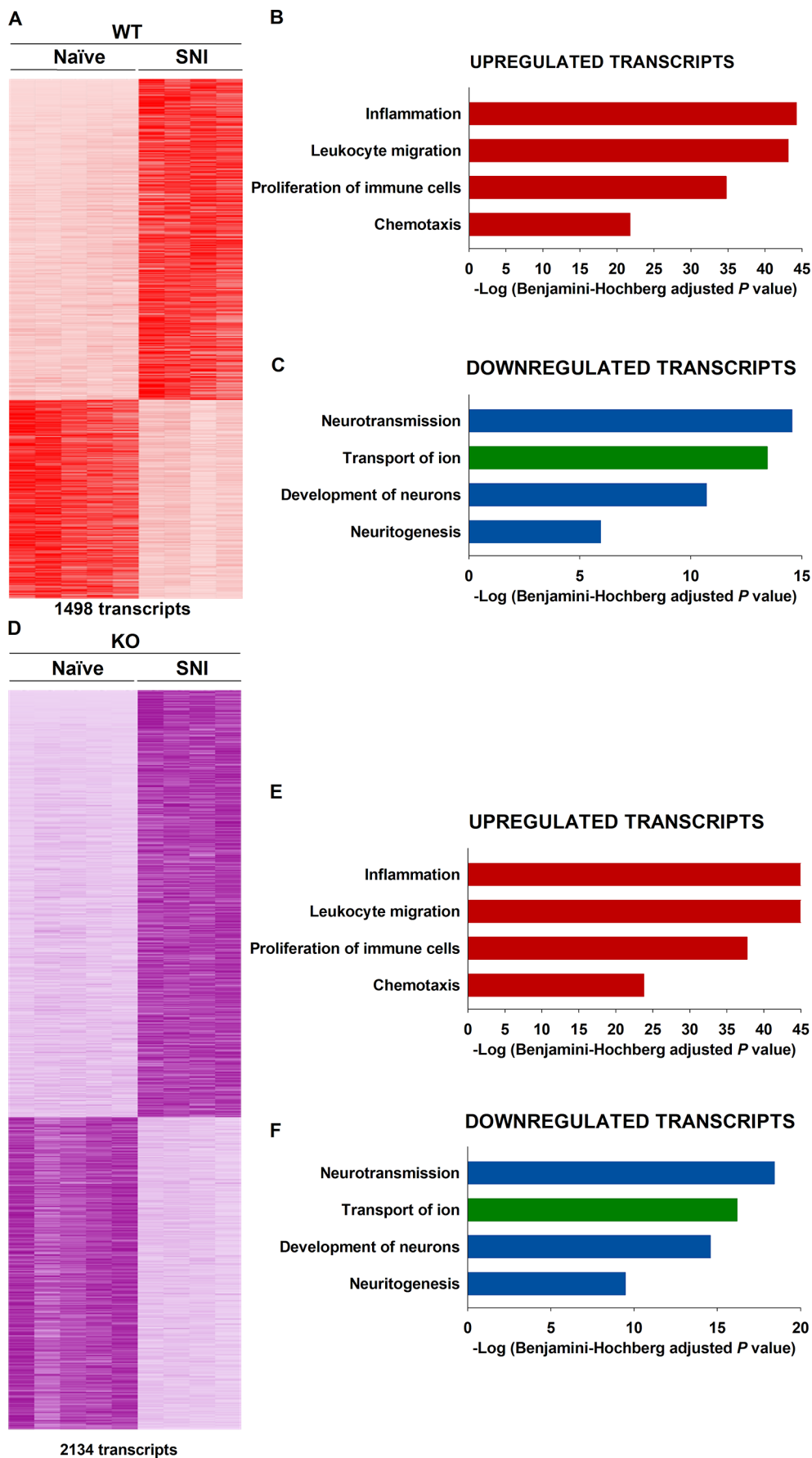
The Regulation of the Transcriptome in the Injured DRG After SNI in WT and Sigma-1 KO Mice Is Broadly Similar

Next, we compared the transcriptional profile of the L3/L4 DRGs from naïve and 7 days post-SNI WT mice. 1498 transcripts were regulated in the injured DRG compared to the naïve condition. A heat map of the regulated transcripts is shown in Fig. 2A. Most of the transcripts regulated in the injured WT DRG increase their expression after SNI (925 transcripts; light to dark red on the heat map), although a significant portion of the transcripts were downregulated (573 transcripts; dark to light red after injury). The transcripts significantly regulated in the DRG from WT mice after SNI are identified in Table S4.

Functional enrichment analysis using the transcripts upregulated after SNI demonstrates a marked enrichment for the annotation of immune functions, with B-H P values close to 10^{-45} (Fig. 2B). The description of the content of the functional annotations of the upregulated transcripts is shown in Table S5. These include cathepsins, chemokines, chemokine receptors, and some well-known immune markers, such as the myeloid marker CD11b, the macrophage/monocyte marker AIF1, or the T cell marker CD4 (among many others). These illustrate the inflammatory process which occurs in the DRG after nerve injury, a process repeatedly described in previous transcriptomic studies (Lacroix-Fralish et al. 2011; Cobos et al. 2018; Ino et al. 2023). In contrast, when the functional enrichment analysis was carried out using the list of downregulated genes, we found that neuronal functions, such as “Neurotransmission”, or “Transport of ion” showed a highly significant B-H P values in the range of 10^{-14} – 10^{-15} (Fig. 2D). The description of the content of the functional annotations of the downregulated transcripts is shown in Table S6. These transcripts include some neurotransmitter receptors but also many different ion channels, such as several potassium, sodium or calcium channels, among many other neuronal-related alterations. All these transcriptional regulations are also extensively documented in previous studies (Davis-Taber and Scott 2006; Du and Gamper 2013; Laedermann et al. 2014).

The association of both immune and neuronal functions to the up- and downregulated gene lists respectively in the DRG after SNI agrees well with previous studies in rodents (Costigan et al. 2010; Cobos et al. 2018) but also in human patients with neuropathic pain (Hall et al. 2022). Interestingly, whereas immune genes are increased by SNI in the WT DRG they are downregulated in the naïve sigma-1 KO mice relative to naïve WT mice. Therefore, in broad terms, the basal transcriptional profile found in the DRG of naïve sigma-1 receptor KO mice is opposite to the changes found

Fig. 2 Transcriptional profile of the injured dorsal root ganglia (DRG) from wild-type (WT) and sigma-1 knockout (KO) mice after spared nerve injury (SNI). **(A)** Heatmap of the relative expression of the transcripts regulated ($P < 0.01$ and a fold change of at least 1.4) in the L3-L4 DRG from WT mice 7 days after SNI compared to naïve mice. Light red represents low-level expression and dark red high-level expression. The total number of regulated transcripts is indicated. **(B-C)** Representative functional characteristics sorted by the strength of statistical significance ($-\log$ of Benjamini-Hochberg adjusted P -value) that IPA software ascribed the function given, using the lists of transcripts **(B)** upregulated or **(C)** downregulated by nerve injury. **(D)** Heatmap of the relative expression of the transcripts regulated in the L3-L4 DRG from KO mice 7 days after SNI compared to naïve mice. Light purple represents low-level expression and dark purple high-level expression. The total number of regulated transcripts is indicated. **(E-F)** Representative functional characteristics sorted by the $-\log$ of Benjamini-Hochberg adjusted P -value ascribed to the function given, using the list of transcripts **(E)** upregulated or **(F)** downregulated by nerve injury



in the DRG after nerve injury in the WT mice, as if the mutant mice exhibit a basal “anti-neuropathic” transcriptomic profile.

Next, we studied SNI induced transcriptional regulation in the L3/4 DRGs of sigma-1 receptor KO mice. We obtained 2134 regulated transcripts in the injured DRG compared to the naïve condition. Most of the transcripts regulated in the injured DRG increase their expression after SNI (1233 transcripts; light to dark purple, Fig. 2D), with 901 transcripts regulated in the opposite direction (dark to light purple Fig. 2D), broadly similar to the changes present in WT mice. The genes significantly regulated in the DRG from sigma-1 receptor KO mice after SNI are identified in Table S7. We conducted a functional enrichment analysis with the lists of transcripts which were up- or downregulated after SNI. Like that described for WT mice after injury, when testing the upregulated transcripts, we found a marked increase in the enrichment for the annotation of immune functions (Fig. 2E), and functional enrichment analysis of downregulated genes yielded a clear predominance of neuronal functions (Fig. 2F). The description of the content of the functional annotations of the up- and downregulated transcripts are shown in Table S8 and S9. The B-H *P* values of all these functions were even more robust than the values seen in WT mice after SNI (compare Fig. 2B-C and E-F), which could be influenced by the altered transcriptional profile found in naïve sigma-1 receptor KO mice, as the baseline in naïve mice is the opposite of the regulation of immune and neuronal transcripts after the SNI, which may amplify the sensitivity of the technique for detecting changes after injury. It can be concluded that the overall immune and neuronal transcriptional alterations induced by nerve injury in the sigma-1 receptor KO mice are like those seen in wild type animals.

Analysis of the Transcriptomic Differences in the DRG from WT and Sigma-1 Receptor KO Mice by WGCNA

As we found broad similarities between the functional groups of genes regulated by SNI in WT or sigma-1 KO mice, we performed a more detailed analysis of differential regulation using a Weighted Gene Co-expression Network Analysis (WGCNA). Here we used those transcripts differentially regulated between either genotype (WT or KO) in the naïve as well as SNI conditions (1259 transcripts).

Following WGCNA analysis, all the regulated transcripts were grouped in 4 clusters attending to their topological overlap in their pattern of regulation (Table S10), with the exception of 9 transcripts that do not belong to any module (Table S11). The heat maps of these modules are shown in Fig. 3A, where light green represents low-level expression

and dark green high-level expression. For clarity, the module eigengenes, as the representative of the gene expression profiles in each module, are shown in Fig. 3B. The similarities between each module are shown in the heat map in Fig. 3C.

It is thought that genes that display similar expression patterns across a wide data set represent groups of functionally interconnected genes (e.g., Horvath et al. 2006; Cobos et al. 2018) and WGCNA groups these genes into modules. Therefore, we performed a functional enrichment analysis for each module. The most significantly associated biological function for each WGCNA module, together with the B-H *P* value and some example genes, is shown in Fig. 3A.

Module I is composed of 436 transcripts. The content of this module is enriched in transcripts related to the functioning of the immune system, as “leukocyte migration” represents its functional annotation (see Fig. 4A). All transcripts associated with this function are shown in Table S12. Expression of these genes is mainly downregulated between the WT and sigma-1 receptor KO under naïve conditions, and their expression remained unchanged after SNI in both genotypes (see Fig. 3A and B). These genes then represent a reduced general immune phenotype in the sigma-1 receptor KO but are not regulated following injury, so likely do not correspond to a differential phenotype following nerve injury.

Module II is topologically close to module I (Fig. 3C), with a Pearson correlation coefficient between both modules of 0.89. However, functional analysis of this group of 547 genes shows that this module is heavily associated with neurotransmission as opposed to module I which is associated with immune genes (Fig. 3A). This result highlights the usefulness of WGCNA to detect subtle differences in the patterns of expression of group of genes with differences in biologically relevant functions. These genes are not regulated by SNI in WT mice, like the transcripts in module I, again suggesting that these genes do not correspond to a differential phenotype following nerve injury. Interestingly, SNI induces changes in expression of these genes in sigma-1 receptor KO mice, which approach to the values of WT mice (Fig. 3A and B). So, module II represents neuronal genes that are mainly high in the naïve KO DRG and downregulated to similar levels to the WT following nerve injury. Again, these genes are likely not relevant to the nerve injury response as they are not regulated in nerve injury in the WT and are normalized by nerve injury in the KO.

Module III is the least populated, with only 44 genes (Fig. 3A), and shows little overlap in the pattern of expression with the other modules (Fig. 3C). Functionally this group is not annotated (Fig. 3A). Here expression is high in the WT naïve with strong downregulation following injury. Expression starts low in the naïve KO and falls

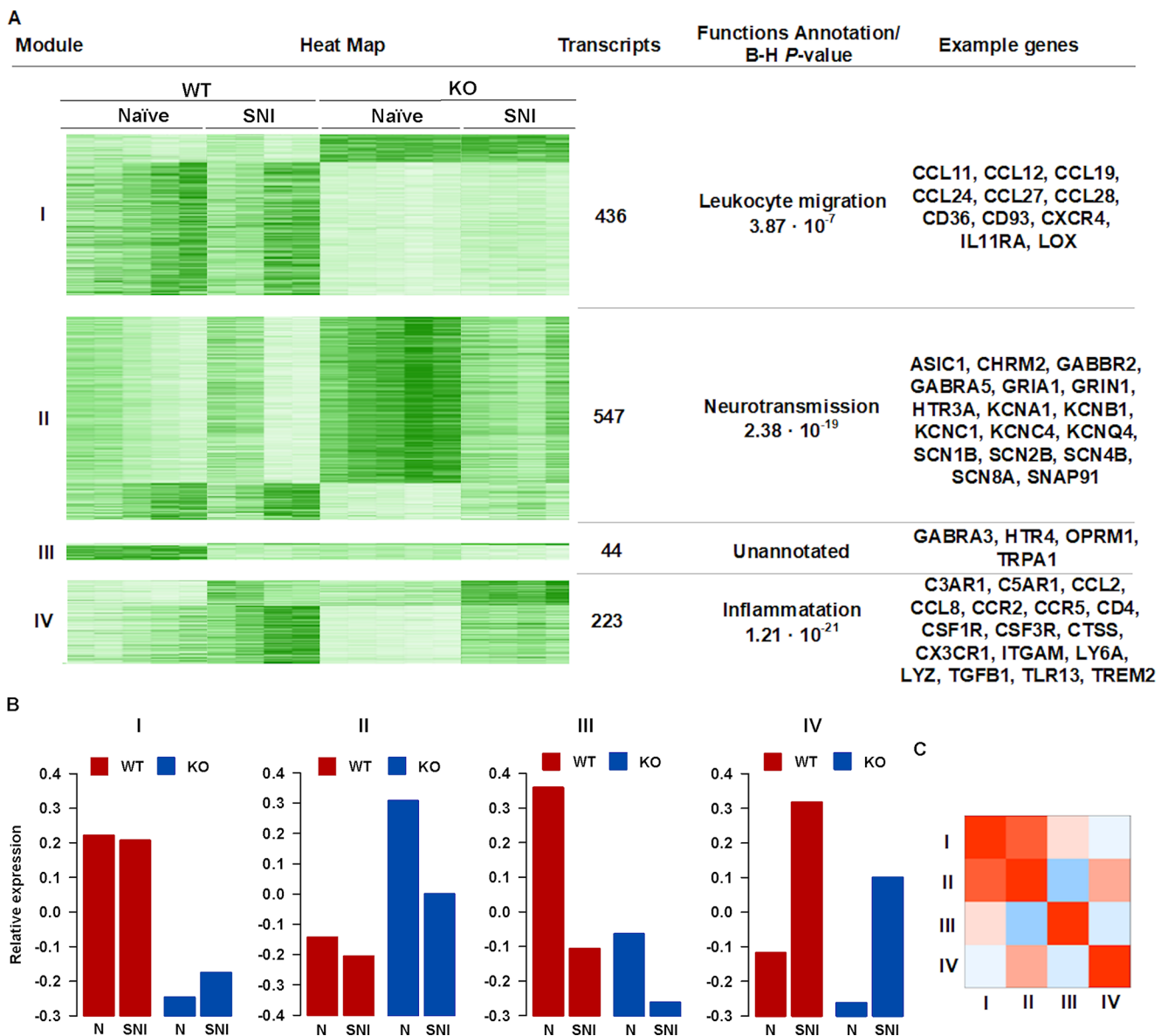


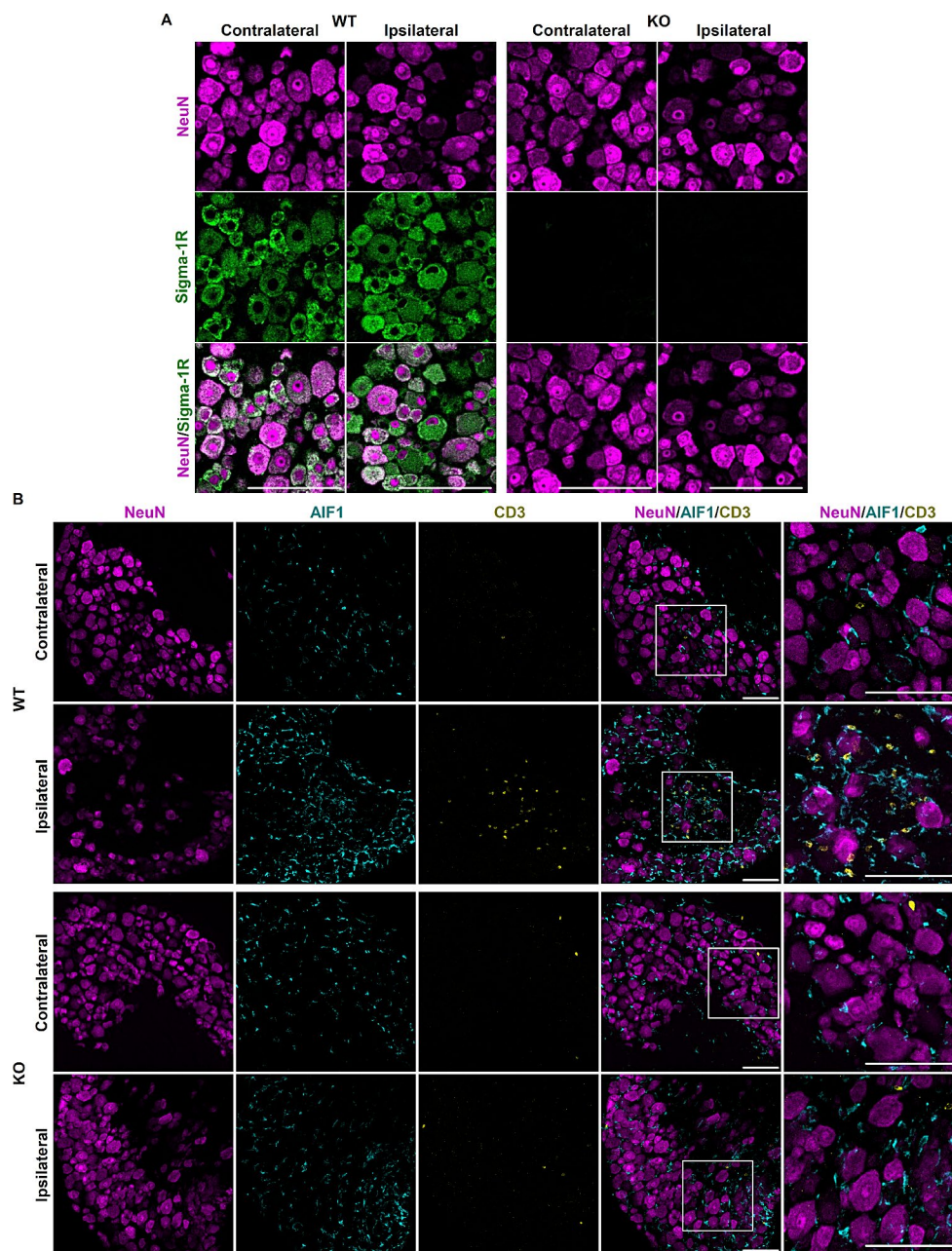
Fig. 3 WGCNA of the transcripts in the dorsal root ganglia (DRG) which are differentially expressed between wild-type (WT) and sigma-1 receptor knockout (KO) mice at either naïve (N) or post-SNI conditions. **(A)** Transcripts from the L3-L4 DRG with significant differences ($P < 0.01$ and a fold change of at least 1.4) between WT and KO mice with or without nerve injury were subjected to WGCNA analysis to produce unbiased modules of coregulated transcripts. The first column defines the module number. The second column shows the heatmaps of the relative expression of each transcript in each module. Light green represents low-level expression and dark green high-level expression. The third column shows the number of transcripts for each

more following nerve injury (Fig. 3A and B). As this group alters following injury the genes may be related to SNI phenotype present in both genotypes. Interestingly there were some genes relevant to neurotransmission inside of this module, such as some receptors for neurotransmitters (GABA and serotonin), and some neuronal genes important

module. The fourth column gives a brief description of module function as defined by IPA software, indicating the Benjamini-Hochberg *P*-value ascribed to the function given, except for module II which could not be identified within any functional category and remained unannotated. The final column gives example transcripts from each functional subdivision. **(B)** Representations of the expression of the eigengenes for modules I-IV, with intensity of regulation on the y axis. Each module contains not only genes regulated in the fashion drawn but also reciprocal regulation events. **(C)** Heatmap of the similarities (adjacencies) in the eigengene network, in which blue color represents low adjacency and red represents high adjacency

for nociception, such as TRPA1 and the OPRM1 (Fig. 3A). OPRM1 or TRPA1 are of note, since both are protein partners of the sigma-1 receptor (Cortés-Montero et al. 2019; Marcotti et al. 2023; Ruiz-Cantero et al. 2023a). The decreased expression of the μ opioid receptor in the naïve sigma-1 KO mice might explain discrepancies between the

Fig. 4 Immunohistochemical changes in the dorsal root ganglia (DRG) of wild-type (WT) and sigma-1 receptor knockout (KO) mice after spared nerve injury (SNI). **(A)** Representative images from the double labeling of NeuN (magenta) and sigma-1 receptor (sigma-1R, green) in L4 DRG contralateral and ipsilateral to the SNI of WT (Left panels) and sigma-1 receptor KO (Right panels) mice, and **(B)** triple labeling of NeuN (magenta), AIF1 (cyan) and CD3 (yellow) in L4 DRG contralateral and ipsilateral to the SNI of WT (Top panels) and sigma-1 receptor KO (Bottom panels) mice. **(A–B)** Samples were obtained 7 days after nerve injury. Scale bars 100 μ m



pharmacological and genetic inhibition of sigma-1 receptors in the modulation of opioid effects (Vidal-Torres et al. 2013; Montilla-García et al. 2018). Downregulation of TRPA1 could help explain the reduction of nociceptive behaviors seen in sigma-1 receptor KO mice after injection of formalin, a known TRPA1 activator, which was the first evidence of the role of sigma-1 receptors on tonic pain (Cendán et al. 2005). Further analysis of this module then may well be of interest in identifying genetic targets intimately involved in the sigma phenotype.

The final module identified by the WGCNA (module IV) was composed of 223 transcripts and shows a distinct pattern of expression that does not overlap with the

other modules (Fig. 3C). This group of genes was heavily enriched in immune-related transcripts, with “Inflammation” the most representative function defined by IPA. Sigma-1 receptor KO mice showed an altered expression (mainly a reduction) of these transcripts in the naïve condition in comparison to WT mice. SNI triggers a prominent upregulation for most transcripts of this module in WT mice (Fig. 3A and B), and therefore may be related to neuropathic pain. Although neuroinflammation is also present in the KO mice following SNI the levels of transcript expression in the SNI DRGs are about equivalent to the WT naïve condition, in summary the neuroinflamed KO DRG has a transcript expression profile similar to the naïve WT DRG.

Module IV contains receptors for complement factors, chemokines, chemokine receptors, cathepsins, and several other immune markers (Fig. 3A). The expression of some of these transcripts is shown in Fig. S2, to exemplify the similarities in their pattern of regulation between these genes. We included chemokines (CCL2 and CCL8), a cathepsin (CTSS), and cytokine receptors and other immune cell markers (CCR5, CX3CR1, TREM2, LY6A, CD4). Altogether, the transcripts in module IV constitute the specific differences between WT and sigma-1 receptor KO mice in the SNI-induced neuroinflammatory process in the DRG. Considering the widely accepted importance of the neuroinflammatory process in the development of neuropathic pain (reviewed in Ji et al. 2014, 2018; Ruiz-Cantero et al. 2021; Ghazisaeidi et al. 2023 and Fig. 2). As well as the attenuation of the expression of these neuroinflammatory markers in the DRG of sigma-1 receptor KO mice following SNI we selected this group for further functional analysis.

CCL8 (alternatively known as monocyte chemoattractant 2, MCP2) is the chemokine with the highest regulation in our dataset in injured WT mice (15-fold) and is also the transcript with the largest fold difference between WT and sigma-1 receptor KO mice during SNI in module IV, with a 7-fold decrease in the sigma-1 receptor KO mice with nerve injury (see second panel in Fig. S2). This cytokine is typically produced by active macrophages (Asano et al. 2015; Halvorsen et al. 2016), although it can also be produced by neurons (Lu et al. 2017). CCL8 acts as a chemotactic factor to attract macrophages but primarily CD4+T cells through interaction with CCR5, which is its canonical receptor (Ruffing et al. 1998; Halvorsen et al. 2016). Interestingly, we found a marked attenuation of the increase of both CCR5 and CD4 in the sigma-1 receptor KO mice in comparison to the robust increase found in WT mice, and in fact, CD4 was not significantly increased in sigma-1 KO mice after SNI (Fig. S2). CCR5 is not the only receptor for CCL8, as it can also bind to CCR3 (Ge et al. 2017). However, the transcript for CCR3 was virtually absent in the DRG samples examined (data not shown). In addition, another transcript with a marked increase after SNI in the WT mice, which was not significantly regulated after injury in the sigma-1 KO mice is LY6A (see Fig. S2), which is also named T-cell-activating-protein (TAP) because of the critical role it plays on T cell activation (Stanford et al. 1997). Therefore, these results suggests that the decrease in some chemokines and other immune cell markers in the injured DRG of sigma-1 receptor KO mice might lead to a reduction of the recruitment of immune cells, including T cells into the DRG following nerve injury.

In summary, the expression patterns of the transcripts with a difference between WT and sigma-1 receptor KO mice, point to a reduced neuroinflammatory process in the

injured DRG of sigma-1 receptor KO mice, which in turn might be participating in the decreased pain phenotype of these mutant mice.

Infiltration of Immune Cells in the Injured DRG of WT and Sigma-1 Receptor KO Mice After SNI

We then studied the expression of sigma-1 receptors in the DRG after SNI. We used immunofluorescence double labeling for sigma-1 receptors and the neuronal marker NeuN in DRGs contralateral and ipsilateral to the nerve injury, in samples from both genotypes obtained 7 days after SNI. In the noninjured DRG from naive WT mice, sigma-1 receptor staining was restricted to NeuN-expressing cells, and all NeuN-expressing cells exhibited sigma-1 receptors staining (Fig. 4A), i.e. sigma-1 receptors had an exclusive neuronal expression, and all neurons expressed sigma-1 receptors. These results are in full agreement with previous studies (Montilla-et al. 2018; Bravo-Caparrós et al. 2020; Shin et al. 2022). In the DRG ipsilateral to SNI, sigma-1 receptor staining was still exclusively present in cells with a neuronal morphology (Fig. 4A). However, some sigma-1 receptor-expressing neurons lost their NeuN labeling in the DRG ipsilateral to SNI (Fig. 4A). This decrease in NeuN staining is known to occur in axotomized neurons (Bravo-Caparrós et al. 2020) and therefore indicates the presence of the DRG neurons injured by the SNI procedure. Importantly, sigma-1 receptor immunostaining was completely absent in either uninjured or injured DRG samples from sigma-1 receptor KO mice (Fig. 4A), indicating the specificity of Sig-1R staining. It can be concluded that the sigma-1 receptor has a neuronal specific distribution in the uninjured or injured DRG.

We aimed to test whether the differences in immune-related transcripts between the DRGs from WT and sigma-1 receptor KO mice detailed in the previous section translate into changes in the presence of immune cells. We investigated by immunohistochemistry the macrophage/monocyte and T cell activation and infiltration into DRG from WT and sigma-1 receptor KO mice. Figure 4B shows representative images for NeuN, the macrophage/monocyte marker AIF1, and the T cell marker CD3 in DRGs contralateral and ipsilateral to the nerve injury, in samples from both genotypes. Little AIF1 staining and virtually no CD3+ cells were detected in the contralateral DRG from either WT or KO animals (Fig. 4B). However, both macrophages/monocytes and T cells were prominently increased in the DRG ipsilateral to the injury in samples from WT mice. Although AIF1+ cells were also present in the injured DRG from sigma-1 receptor KO animals, their presence was significantly diminished relative to the WT injured DRG. CD3+ cells were virtually

absent in the injured DRGs of the KO mice like that seen in the contralateral (Fig. 4B).

We next quantified by FACS the presence of immune cells in DRGs from uninjured and injured WT and sigma-1 receptor KO mice. We determined neutrophils (CD45 + CD11b + Ly6G + cells), macrophages/monocytes (CD45 + CD11b + Ly6G – cells), B cells (CD45 + CD45R/B220+), and T cells (CD45 + TCR β +). Although in previous sections we found a lower expression in immune transcripts in naïve sigma-1 receptor KO mice in comparison to naïve WT mice, this did not translate into a decrease in the presence of any of the immune cells tested (see Fig. 5A-C), likely because of sensitivity differences between the methods, with FACS being less sensitive than RNAseq, in particular during the naïve condition, where the number of resident immune cells in the DRG is low. We also examined whether the sham procedure has an impact in the recruitment of immune cells into the DRG, and found a virtually identical presence of neutrophils, macrophages/monocytes, B cells, and T cells than in samples from sham or naïve animals (see the “Ipsilateral” values in Fig. 5A-C).

Next, we examined the infiltration of immune cells into the injured DRGs in WT mice and whether sigma-1 receptor KO mice had an alteration in this process. Neutrophils are not significantly recruited in the DRG ipsilateral to SNI from either WT or sigma-1 receptor KO mice (see the “Ipsilateral” values in Fig. 5A). These data agree with previous studies which show that neutrophils do not participate in the neuroinflammatory process after SNI (Lindborg et al. 2018; Bravo-Caparrós et al. 2020). On the other hand, we found a marked increase in the presence of macrophages/monocytes in the injured DRG from WT mice on day 7 after SNI, compared to the values found on the DRG from naïve animals. This increase was partially attenuated in sigma-1 receptor KO mice (see the “Ipsilateral” values in Fig. 5A) supporting our previous data where macrophage/monocyte infiltration and or activation in the DRG after SNI is decreased by sigma-1 receptor inhibition, purportedly by the decrease in the production of CCL2 (Bravo-Caparrós et al. 2020).

We also examined the presence of relevant lymphocyte lineages in the DRG from WT and sigma-1 receptor KO mice before and after nerve injury. B cells did not significantly increase in the injured DRG from animals of either genotype (see the “Ipsilateral” values in Fig. 5B). Therefore, this immune cell type does not appear to participate in SNI-induced neuropathic pain, as previously reported (Cobos et al. 2018). On the other hand, the number of T cells significantly increased in the DRG ipsilateral to nerve injury of WT mice, and importantly sigma-1 receptor KO mice did not show any apparent increase in the presence of this cell type in the injured DRG (see the “Ipsilateral” measures in Fig. 5B). Further analysis explored the contribution of

CD4+ and CD8+ subpopulations of T cells. We found that the recruitment of CD4+ T cells in the DRG from WT was considerably larger than the increase in CD8+, which was modest (see the “Ipsilateral” values in Fig. 5C). Sigma-1 receptor KO mice did not show any increase in any of these T cell subpopulations in the injured DRG (see the “Ipsilateral” values in Fig. 5C).

We also examined the DRGs contralateral to SNI, but we did not find any increase in any immune cell population explored in comparison to the values found in naïve animals (see the “Contralateral” measures in Fig. 5A-C).

In summary, although sigma-1 receptors have a neuronal specific distribution in the DRG, they have an impact on immune cell recruitment after SNI. To our knowledge, this is the first report showing that sigma-1 receptor KO has an influence on T cell recruitment in the DRG after nerve injury. The effect of sigma-1 KO was proportionally more robust on CD4+ T cells than on any other immune cell type explored, as it completely blocked the infiltration of this immune cell type into the DRG. Although CD4+ T cells have a lower presence than myeloid cells in the peripheral neuroinflammatory response of neuropathic animals, it is thought that CD4+ T cells orchestrate the immune response and play a pivotal role in the development of neuropathic pain in the DRG (Vicuña et al. 2015; Cobos et al. 2018; Chen et al. 2022; Ino et al. 2023). Therefore, it could be hypothesized that the absence in the recruitment of CD4+ T cells into the DRG of our mutant mice might have an impact in their reduced pain phenotype.

Infiltration of Immune Cells in the Paw of WT and Sigma-1 Receptor KO Mice After CFA-Induced Inflammation

Since sigma-1 receptor KO mice showed a decrease in the recruitment of immune cells in the injured DRG after SNI, we aimed to test whether these mutant mice had a generalized deficit in the production or recruitment of immune cells that would account for the decrease in the neuroinflammatory process observed. Therefore, we evaluated immune cell recruitment in the inflamed paw induced by CFA.

The number of resident immune cells in the paw tissue from naïve WT or sigma-1 receptor KO was indistinguishable. These include neutrophils (Fig. 6A), macrophages/monocytes (Fig. 6A), B cells (Fig. 6B), and T cells (Fig. 6B), including the CD4+ (Fig. 6C) and CD8+ (Fig. 6C) subpopulations.

We then examined the presence of these immune cells in the paws from mice injected with CFA (10–20 μ L) or with saline (20 μ L). Saline injection did not alter the presence of any of the immune cells tested in comparison to the naïve values (see the “Ipsilateral” values in Fig. 6A-C). However,

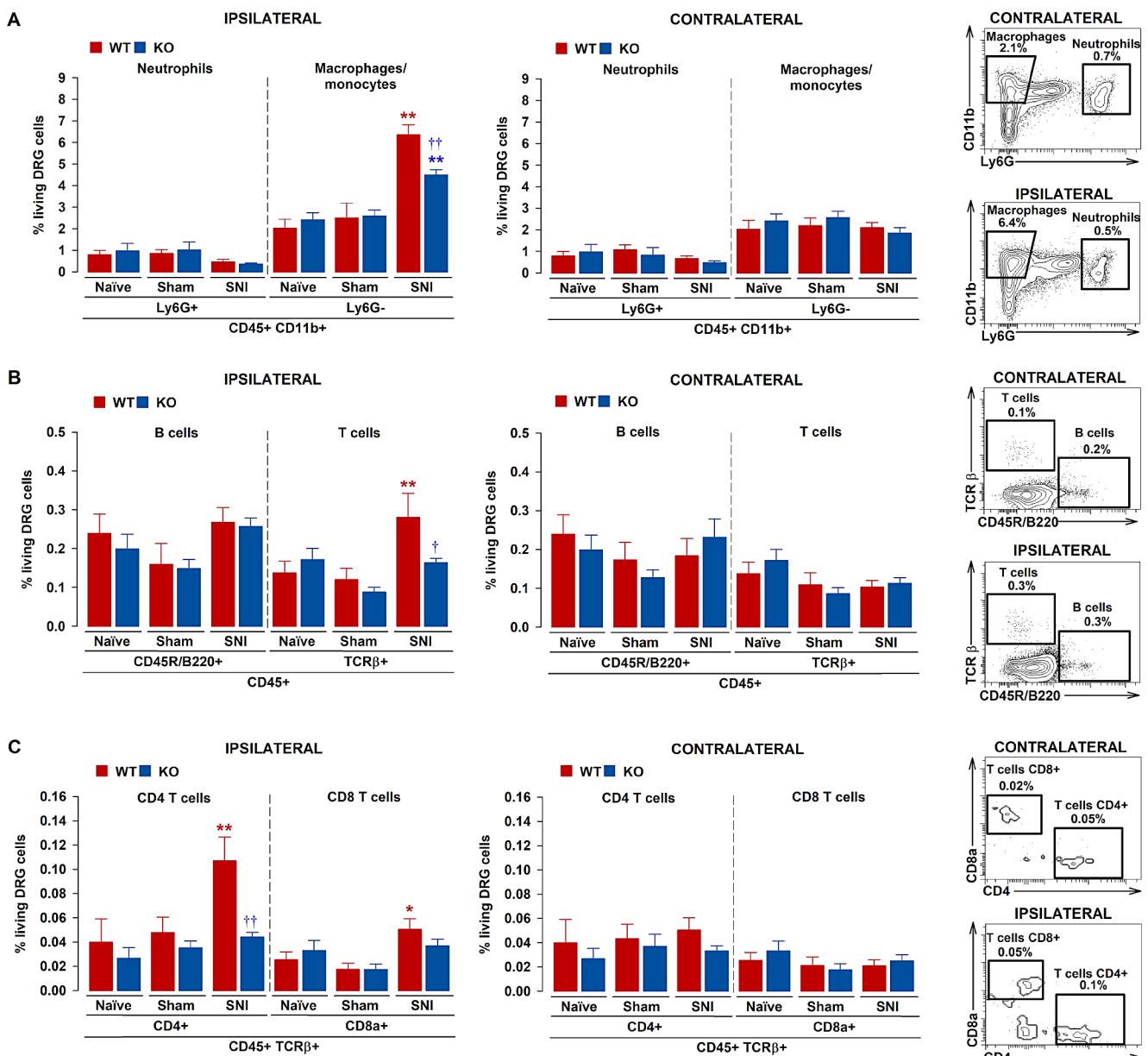


Fig. 5 Infiltration of immune cells in the injured dorsal root ganglia (DRG) of wild-type (WT) and sigma-1 receptor knock-out (KO) mice after spared nerve injury (SNI). Quantification of (A) Neutrophils (CD45 + CD11b + Ly6G + cells) and macrophages/monocytes (CD45 + CD11b + Ly6G – cells), (B) B cells (CD45 + CD45R/B220 +) and T cells (CD45 + TCRβ + cells), and (C) CD4 T cells (CD45 + TCRβ + CD4 + cells) and CD8 T cells (CD45 + TCRβ + CD8a + cells) determined by FACS in the DRG from naïve mice, and ipsilateral and contralateral DRG from mice with SNI or sham-operated mice 7 days after surgery. For the naïve group, the values from the left and right side were averaged as there were no dif-

ferences between them. Representative FACS diagrams, gated from CD45 + cells, and obtained from the DRG ipsilateral and contralateral to the SNI of WT mice, are shown beside the quantification of the several immune cell types. (A–C) Each bar and vertical line represent the mean ± SEM of the values obtained in 7–10 batches of L3–L4 DRG. Statistically significant differences between the values in naïve and SNI ipsilateral groups within samples from the same genotype: ** $P < 0.01$, * $P < 0.05$ and between DRG ipsilateral to SNI in the WT and KO groups: †† $P < 0.01$, † $P < 0.05$ (two-way ANOVA followed by Student–Newman–Keuls)

the administration of CFA induced a robust increase in neutrophils and macrophages/monocytes in the injected paw of both WT and sigma-1 receptor KO mice. A dose-dependent effect was particularly appreciated in neutrophil recruitment. The increase in these immune cells was equally robust in WT

or sigma-1 receptor KO mice (see the “Ipsilateral” measures in Fig. 6A). We also studied the presence of lymphocyte lineages during CFA-induced inflammation. We did not detect a statistically significant increase in B cells after CFA injection in mice from either genotype, but we found a prominent

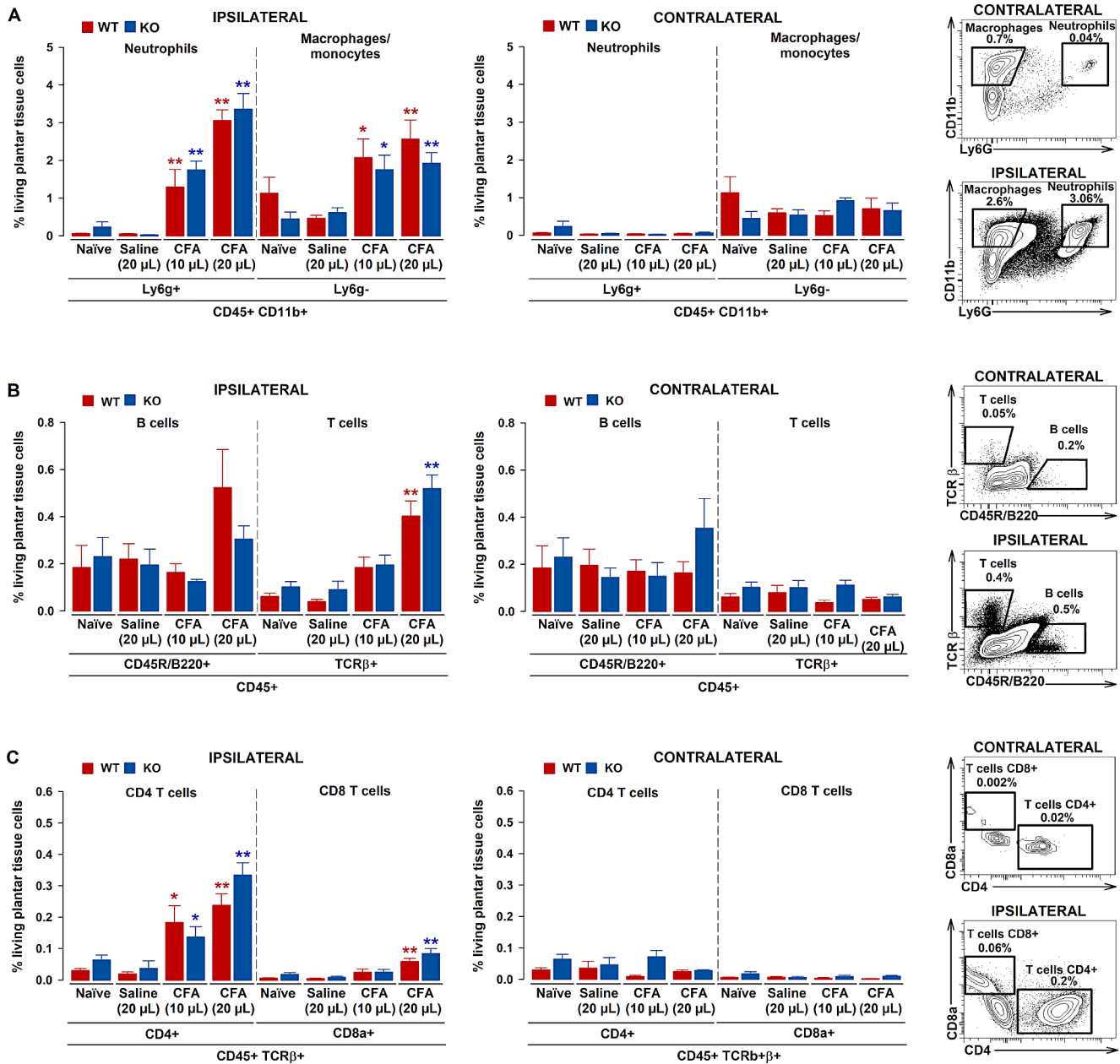


Fig. 6 Infiltration of immune cells in the paw of wild-type (WT) and sigma-1 receptor knockout (KO) mice after peripheral inflammation induced by the intraplantar administration of Complete Freund's Adjuvant (CFA). (A) Neutrophils (CD45 + CD11b + Ly6G + cells) and macrophages/monocytes (CD45 + CD11b + Ly6G – cells), (B) B cells (CD45 + CD45R/B220+) and T cells (CD45 + TCRβ + cells), (C) CD4 T cells (CD45 + TCRβ + CD4 + cells) and CD8 T cells (CD45 + TCRβ + CD8a + cells) were determined by FACS in plantar tissue from naïve mice, and ipsilateral and contralateral plantar tissue from mice 7 days after with CFA-induced inflammation. For the naïve

group, the values from the left and right paw were averaged as there were no differences between them. Representative FACS diagrams, gated from CD45 + cells, and obtained from the paw ipsilateral and contralateral to the inflammation induced by CFA 20 µL in WT mice, are shown beside the quantification of the several immune cell types. Each bar and vertical line represent the mean ± SEM of the values obtained from 7–10 independent paw samples. Statistically significant differences between the values in naïve and CFA ipsilateral groups within samples from the same genotype: ** $P < 0.01$, * $P < 0.05$ (two-way ANOVA followed by Student-Newman-Keuls)

and dose-dependent increase in T cell recruitment in the inflamed paw, which was of a similar magnitude in WT and sigma-1 receptor KO mice (see the “Ipsilateral” measures in Fig. 6B). We also studied the CD4 + and CD8 + subpopulations of T cells and found that both were dose-dependently

and significantly increased in the inflamed paw, and to a similar extent in both genotypes (see the “Ipsilateral” measures in Fig. 6B). Therefore, sigma-1 receptor KO mice do not show any apparent deficit in immune cell recruitment in response to paw inflammation. We did not find statistically

significant differences in the immune cell populations in the paws contralateral to the injection of saline or CFA in comparison to the values found in naïve animals (see the “Contralateral” measures in Fig. 6A-C).

It can be concluded that the decrease in immune cell infiltration in the DRG of sigma-1 receptor KO mice described in the previous sections cannot be explained by an overt deficit in the immune response of these mutant animals, and taking into account the neuronal selective distribution of sigma-1 receptors in the DRG, our findings rather suggest that is a mechanism related to the neuronal regulation of immune cell trafficking in the DRG.

The Behavioral Phenotype of Sigma-1 Receptor KO Mice in SNI-Induced Neuropathic Pain Is Partially Replicated by Treatment with Maraviroc

To determine if the changes in immune cell recruitment have any effect on the behavior of the sigma-1 receptor KO mice relative to WT we assayed mechanical and cold hypersensitivity in these mice, as well as spontaneous pain-like responses. We compared the behavioral results of sigma-1 KO mice with those obtained in WT mice treated with maraviroc. Maraviroc is a specific inhibitor of CD4+ T cells and operates as a CCR5 antagonist (Rosario et al. 2008).

We initially compared the response to mechanical stimulation of WT and sigma-1 receptor KO mice before and after SNI. Baseline mechanical threshold in von Frey test did not significantly differ between naïve genotypes (Fig. 7A). One week post SNI, WT mice developed mechanical allodynia in their injured paw ipsilateral to the SNI. Sigma-1 receptor KO mice also showed mechanical hypersensitivity after SNI although it was significantly less pronounced than WT mice (Fig. 7A). The responses to mechanical stimulation remained unchanged in the paw contralateral to the nerve injury in WT or sigma-1 receptor KO mice (Fig. 7A). No change was observed in the mechanical thresholds in sham-operated mice from either genotype (Fig. S3A).

It has been reported that spinal microglia play a more prominent role on neuropathic mechanical allodynia in male than in female mice, whereas central T cells play a more active role in female than in male animals (Sorge et al. 2015). We previously reported that SNI-induced mechanical allodynia could be efficiently attenuated by inhibition of either macrophages or T cells in male mice, purportedly by peripheral mechanisms (Cobos et al. 2018). Our current results showing a decrease in peripheral neuroinflammation and tactile allodynia in female sigma-1 KO mice seems to mimic the effect of the peripheral immune cell inhibition seen in male mice. Nevertheless, it would be of interest to design a study to specifically test whether the sexual dimorphism of central neuroinflammation in pain can be applied

or not to the peripheral neuroinflammatory response. The effects of sigma-1 inhibition in mice from both sexes has been previously compared under several pain conditions, and it was found male and female sigma-1 KO mice experienced a virtually identical decrease in neuropathic hypersensitivity after SNI (Bravo-Caparrós et al. 2019). In addition, pain sensitization by the injection of chemical algogens such as capsaicin and prostaglandin E2 is equally attenuated by sigma-1 inhibition in both sexes (Entrena et al. 2009; Ruiz-Cantero et al. 2023a). Therefore, although there is clear sexual dimorphism in certain pain mechanisms, up to now there is no evidence for such differences regarding the modulatory role of sigma-1 receptors in pain.

Although in the present study sample collections and behavioral assays were made 7 days after SNI, we previously reported that the difference in sensory hypersensitivity between WT and sigma-1 KO mice is maintained for at least 21 days (Bravo-Caparrós et al. 2019). Therefore, it can be speculated that the attenuated neuroinflammatory response seen here in sigma-1 KO mice would be not restricted to 7 days but maintained for a longer period to sustain these behavioral differences.

As we found that the attenuated neuropathic hypersensitivity seen in sigma-1 receptor KO mice is accompanied by a reduction in peripheral neuroinflammation, including a marked decrease in the recruitment of CD4+ T cells into the DRG (Fig. 5C), we attempted to mimic the effect of sigma-1 receptor inhibition by treatment with maraviroc. As expected, control mice treated with the solvent of maraviroc showed a marked decrease in the mechanical threshold of the injured paw 7 days after SNI (Fig. 7B). SNI mice treated during 7 days with maraviroc in the drinking water showed a significant recovery of the mechanical threshold in the paw ipsilateral to the surgery (Fig. 7B), and to the same extent that the antiallodynic effect seen in sigma-1 KO mice (compare Fig. 7A and B). Therefore, pharmacological antagonism of CCR5 and T cell actions in WT mice mirrored the effect of sigma-1 KO mice in tactile allodynia. The effect of maraviroc was restricted to the injured paw as the mechanical threshold of the contralateral paw was virtually identical to the baseline measure (Fig. 7B). Therefore, maraviroc did not induce a broad increase in the mechanical threshold of the mice but a specific anti-allodynic effect.

We also tested sensitivity to cold stimulation using an acetone drop. Baseline responses to acetone were equal in naïve WT and sigma-1 receptor KO mice with a minimal response (licking/biting the paw) (Fig. 7C). One week after SNI, WT mice developed marked cold allodynia in the injured limb, with a duration of paw licking/biting of about 12 s. In contrast, sigma-1 receptor KO mice had a minimal cold hypersensitivity, showing only a modest increase (2.4 s) in the behavioral response (Fig. 7C). The responses

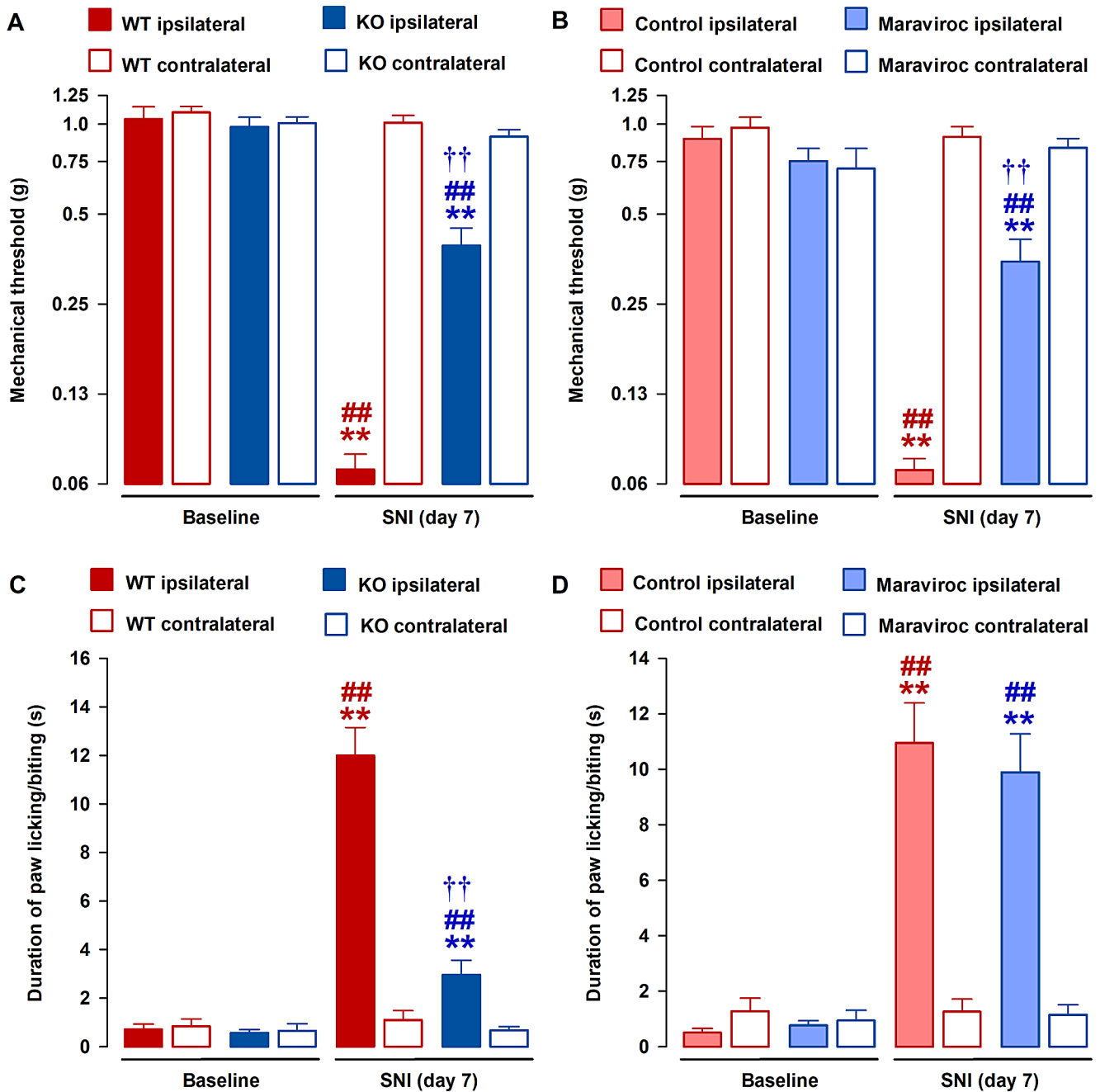


Fig. 7 Reduction of sensory hypersensitivity in sigma-1 receptor knockout (KO) mice after spared nerve injury (SNI) is partially replicated in wild-type (WT) mice treated with maraviroc. The von Frey threshold (A and B) and duration of hind paw licking or biting in the acetone test (C and D) were recorded before the injury (baseline) and 7 days after SNI in the paws ipsilateral and contralateral to the site of surgery. We compared behavioral responses in WT and sigma-1 receptor KO mice (A and C) and in WT mice treated with maraviroc or its solvent (B and D). Maraviroc was dissolved at 300 mg/L in the drinking water, which results in an approximate dose of 50 mg/kg/day (see

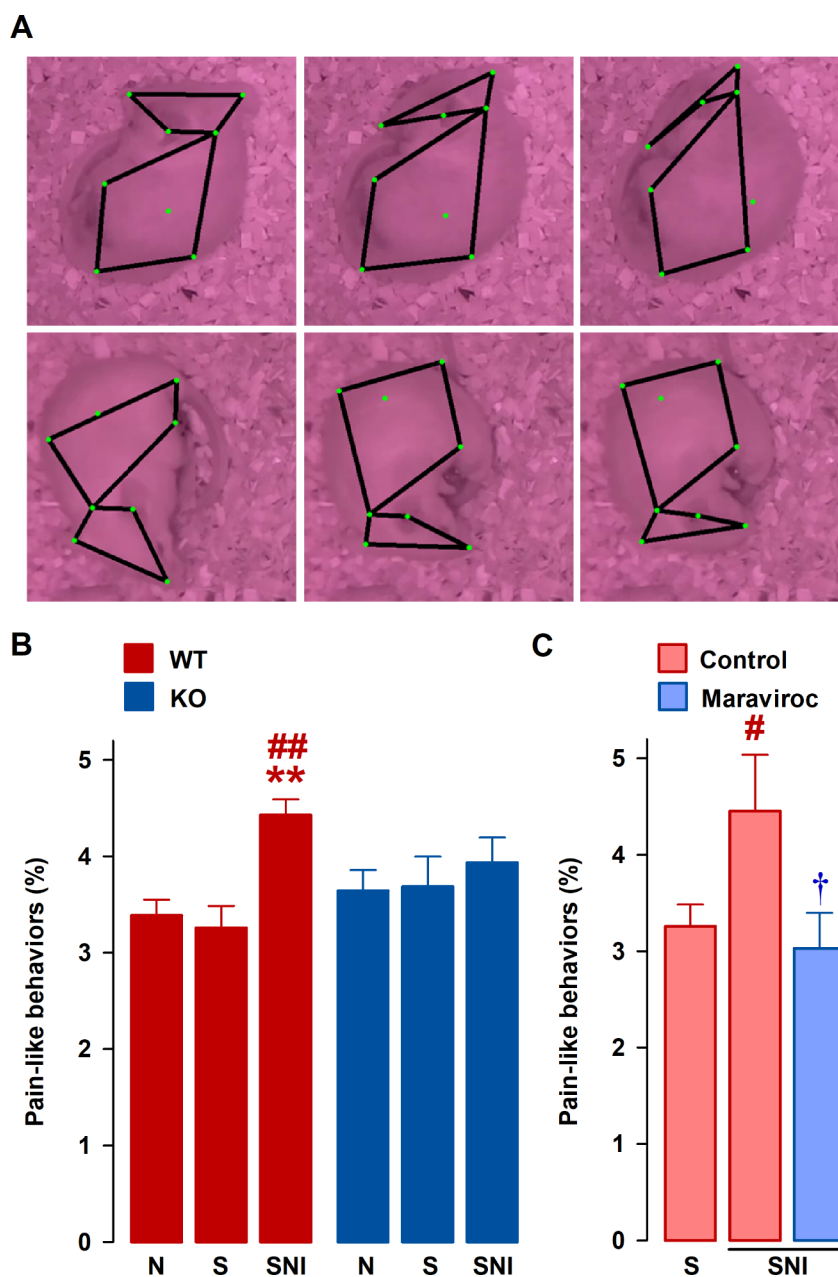
Methods for details) and was given to the mice from the day before the SNI until the day of the sensory evaluation. Control mice were given drinking water without any additives. Each bar and vertical line represent the mean ± SEM of the values obtained in 10–12 animals. Statistically significant differences between the values obtained in the ipsilateral paw on the baseline and day 7 after SNI: ** $P < 0.01$; between the ipsilateral and contralateral measurements: ## $P < 0.01$; and between WT and KO groups or control and maraviroc-treated mice stimulated in the paw ipsilateral to SNI: †† $P < 0.01$ (two-way repeated measures ANOVA followed by Student-Newman-Keuls)

to cold stimulation remained unchanged in the paw contralateral to the nerve injury in WT or sigma-1 receptor KO mice (Fig. 7C). No change was observed in the responses to acetone in sham-operated mice from either genotype (Fig. S3B). Interestingly, treatment with maraviroc was unable to alter the behavioral responses to acetone (licking/biting the paw) in either the injured or the uninjured paw, and mice still showed a marked cold allodynia in the paw ipsilateral to the SNI (Fig. 7D). Therefore, although maraviroc could replicate the effect of sigma-1 inhibition in the responses to mechanical stimulation, it was unable to do so when a cold stimulus was used.

In addition to cutaneous hypersensitivity, we also evaluated spontaneous pain-like behaviors in mice after SNI.

Fig. 8 Reduction in spontaneous pain-like responses of sigma-1 receptor knockout (KO) mice after spared nerve injury (SNI) is replicated in wild-type (WT) mice treated with maraviroc. **(A)** Representative sequence of three frames of a pain-like response episode identified by the algorithm in two different mice. Points and lines represent some key anatomical features of each animal that were automatically identified to calculate their coordinates and hence the postures of the animals. **(B)** The duration of spontaneous pain-like responses (% of frames in the 48-h recording – starting after day 7 post-SNI) was estimated in WT and sigma-KO mice in naïve (N), sham (S) or SNI conditions. **(C)** Spontaneous pain-like responses were assessed in sham (S) or SNI WT mice treated with maraviroc or its solvent. Maraviroc was dissolved at 300 mg/L in the drinking water, which results in an approximate dose of 50 mg/kg/day (see Methods for details) and was given to the mice from the day before the SNI until the last day of the recording. SNI control mice were given drinking water without any additives. Each bar and vertical line represent the mean \pm SEM of the values obtained in 12–20 animals. Statistically significant differences between the values in naïve and SNI groups within samples from the same genotype: $**P < 0.01$; between the values in sham and SNI groups: $\#P < 0.05$, $\#\#P < 0.01$; and between control and maraviroc-treated mice with SNI: $\dagger P < 0.05$, $\dagger\dagger P < 0.01$ (two-way ANOVA followed by Student-Newman-Keuls)

We first interrogated the K-Means algorithm to group the behaviors of 48-h recordings of naïve and SNI WT mice in an unsupervised manner, and we selected asymmetrically directed behaviors that involved the approach of the head of the animal to the injured limb as spontaneous pain-like behaviors (see Methods for details). Figure 8A shows a sequence of three frames of a spontaneous pain-like episode identified by the algorithm in two different mice. The duration of these pain-like responses significantly increased from $3.39 \pm 0.16\%$ in naïve mice to $4.42 \pm 0.16\%$ in SNI mice, as shown in Fig. 8B. It has been reported that these types of asymmetric behaviors are too rare to be considered as representing spontaneous pain (Mogil et al. 2010). However, typical evaluations



performed by human observers are made during a very limited time (usually in recordings not longer than 60 min) (e.g. Mogil et al. 2010). Our study shows that the automatic evaluation of these behaviors by a (tireless) algorithm allows days-long recordings to be monitored with well-defined and invariant instructions, and even if pain-like responses occur with a very low frequency, they can be objectively quantified to study spontaneous pain, since they significantly increase in neuropathic mice.

We then used the K-Means algorithm to identify these pain-like responses in other experimental groups. We found that sham mice showed values indistinguishable from those of naïve animals (Fig. 8B). Then, we explored these behaviors in uninjured (naïve or sham) or SNI sigma-1 KO mice. There were no differences between the values found in these three groups of mutant animals, which were similar to the values from uninjured WT mice (Fig. 8B). Finally, we also studied the effect of maraviroc treatment on spontaneous pain-like behaviors during neuropathic pain. When we applied the algorithm to new groups of sham and SNI WT mice, we found again an increase in pain-like behaviors in neuropathic animals, indicating the robustness of the detection of these behaviors. The increase in pain-like responses seen in SNI mice was abolished by treatment with maraviroc (Fig. 8C). This is, to our knowledge, the first study which shows a decrease in neuropathic spontaneous pain-like behaviors by sigma-1 KO or by maraviroc treatment.

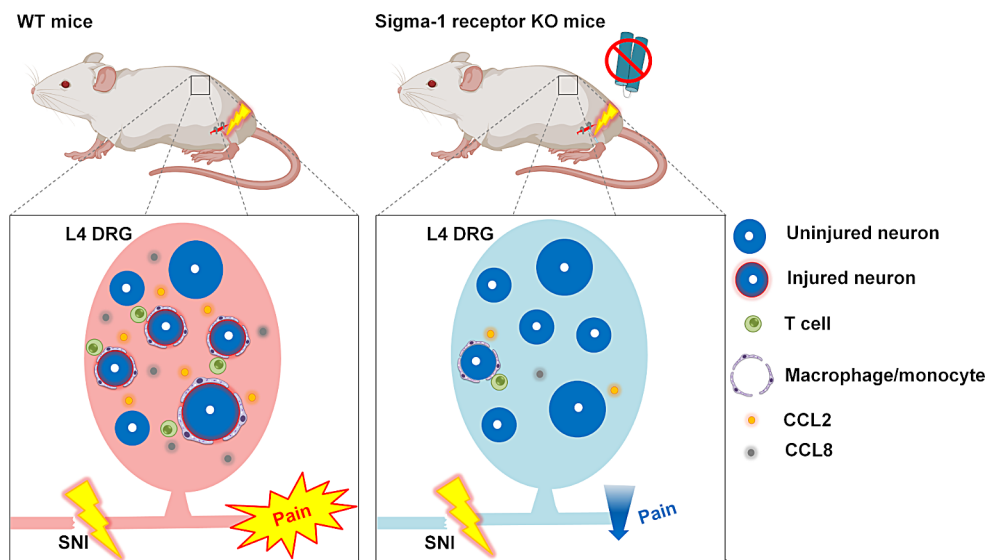
Maraviroc is used in the treatment of the infection caused by the human immunodeficiency virus (HIV). The dose used in our study in mice (50 mg/kg/day) theoretically translates to a dose approximately equivalent to 300 mg/day in humans considering an interspecies allometric scaling factor of 12.3, following the recommendations by FDA (Nair and Jacob 2016), which is within the therapeutic range of this drug (Gulick et al. 2008). Our results would support an additional indication of maraviroc, at doses normally used in therapy, to ameliorate (at least some symptoms associated with) neuropathic pain. There are only two previously published studies which tested the effects of maraviroc on neuropathic sensory

hypersensitivity, and both studies administered this drug intrathecally (Kwiatkowski et al. 2016; Piotrowska et al. 2016). Here we show for the first time that oral administration is enough to induce an effect in tactile allodynia but also in spontaneous pain-like behaviors. Considering that this drug is known to have a very limited central permeability (Garvey et al. 2012) it is reasonable to hypothesize that these effects are produced peripherally.

In spite of the robust effect of maraviroc in tactile allodynia or spontaneous pain-like responses, our data suggest that pharmacological inhibition of T cell actions during neuropathic pain is not enough to decrease cold allodynia. The absence of effect of maraviroc treatment on cold allodynia in female animals is consistent with previously published data where the depletion of T cells in male mice did not affect cold hypersensitivity and suggests that cold allodynia develops from changes in sensory neurons in a manner independent of the participation of these immune cells in either female (this study) or male (Cobos et al. 2018) mice. Therefore, the robust decrease of cold allodynia seen in the sigma-1 KO mice cannot be attributed to the decreased peripheral neuroinflammatory process but to independent neuronal effects. It has been described that sigma-1 receptor is a modulator of TRPs, including TRPV1 (Cortés-Montero et al. 2019; Ruiz-Cantero et al. 2023a), TRPM8 and TRPA1 (Cortés-Montero et al. 2019). In fact, it has recently been shown that TRPA1 modulation by sigma-1 receptor has a strong impact on oxaliplatin-induced cold allodynia (Marcotti et al. 2023). Therefore, it is tempting to speculate that the direct modulatory effects of sigma-1 receptors on TRPA1 (maybe in conjunction to other ion channels) might produce the amelioration of SNI-induced cold allodynia in a manner independent of the neuroinflammatory process.

Finally, although our results suggest that DRG sigma-1 receptors play a role in neuropathic pain, we cannot rule out the simultaneous participation of sigma-1 receptors in central nervous system, since it is known that sigma-1 receptors can also modulate neurotransmission in the spinal cord and pain-related supraspinal areas (Merlos et al. 2017; Ruiz-Cantero et al. 2021).

Fig. 9 Proposed actions for the effects of sigma-1 receptor on dorsal root ganglia (DRGs) neuroinflammation after spared nerve injury (SNI). In wild-type (WT) mice, injured DRGs exhibits high levels of CCL8, CCL2 (among other cytokines) and a massive infiltration of macrophages/monocytes and T cells, which favors neuropathic pain development. In contrast, sigma-1 receptor knockout (KO) mice showed reduced levels of CCL2 and CCL8, decreased macrophage/monocyte infiltration and a negligible presence of T cells into DRGs, together with a reduced neuropathic pain phenotype after SNI. The mouse drawing was obtained from BioRender.com



Conclusions

In summary, our data indicate that peripheral sigma-1 receptors play a pivotal role in the communication between peripheral sensory neurons and the immune system after nerve injury. Sigma-1 inhibition decreases the recruitment and activation of macrophages/monocytes and CD4+T cells in the injured DRG, at least in part through the reduction in the production of several cytokines such as CCL2 or CCL8 (Fig. 9). This effect is not due to a broad immunomodulatory effect of sigma-1 receptors, as no apparent decrease in immune cell recruitment in an inflamed paw is observed after local injection of an inflammatory agent. Modulation of DRG neuroinflammation by sigma-1 receptors might partially explain the amelioration of neuropathic tactile allodynia and spontaneous pain-like responses seen in sigma-1 receptor KO mice, but it cannot explain the effect on cold allodynia. Therefore, sigma-1 receptor inhibition may be potentially effective to decrease neuropathic pain through the inhibition of peripheral neuroinflammation and additional mechanisms.

Supplementary Information The online version contains supplementary material available at <https://doi.org/10.1007/s11481-024-10144-8>.

Acknowledgements We thank Sara Moreno San Juan (Microscopy and Cellular Imaging Unit - ibs.GRANADA) for her technical support with confocal microscopic image acquisition, Adrián García-Moreno and Luis Javier Martínez (Bioinformatics and Genomics Units from the Centre for Genomics and Oncological Research - GENyO) for their support with the bioinformatic analyses, and Gustavo Ortiz Ferrón (Flow Cytometry Unit, Centre for Scientific Instrumentation, University of Granada) for his technical support in the FACs experiments. This research was done in partial fulfilment of the requirements for the doctoral thesis of M.C. Ruiz-Cantero.

Author Contributions Enrique J. Cobos, Rafael González-Cano and M. Carmen Ruiz-Cantero designed research; M. Carmen Ruiz-Cantero, Rafael González-Cano, José M. Entrena, Antonia Artacho-Cordón and Miguel Á. Huerta performed research; M. Carmen Ruiz-Cantero, Rafael González-Cano, José M. Entrena, Enrique Portillo-Salido, Francisco R. Nieto and Enrique J. Cobos analyzed data; and M. Carmen Ruiz-Cantero, José M. Baeyens, Rafael González-Cano, Michael Costigan and Enrique J. Cobos wrote the paper.

Funding This study was partially supported by the Spanish State Research Agency (<https://doi.org/10.13039/501100011033>) under the auspices of the Spanish Ministry of Science and Innovation (MCIN, grant numbers SAF2016-80540-R and PID2019-108691RB-I00), the Andalusian Regional Government (grant CTS-109), and the European Regional Development Fund. M.C. Ruiz-Cantero and M.Á. Huerta were supported by the Training University Lecturers program (FPU16/03213 and FPU21/02736, respectively) of the Spanish Ministry of Universities. The authors also thank the support of the Unit of Excellence 'UNETE' from the University of Granada (reference UCE-PP2017-05).

Data Availability Expression data can be found in Gene Expression Omnibus (GEO) database, with accession number GSE241361.

Declarations

Ethical Approval Mice were handled in accordance with international standards (European Communities Council directive 2010/63), and the experimental protocols were approved by regional (Junta de Andalucía) and Institutional (Research Ethics Committee of the University of Granada) authorities.

Consent for Publication The manuscript has been approved by all authors.

Conflicts of Interest/Competing Interests The authors declare that there are no conflicts of interest.

References

- Asano K, Takahashi N, Ushiki M et al (2015) Intestinal CD169(+) macrophages initiate mucosal inflammation by secreting CCL8 that recruits inflammatory monocytes. *Nat Commun* 6:7802. <https://doi.org/10.1038/NCOMMS8802>
- Bravo-Caparrós I, Perazzoli G, Yeste S et al (2019) Sigma-1 receptor inhibition reduces neuropathic pain induced by partial sciatic nerve transection in mice by opioid-dependent and -independent mechanisms. *Front Pharmacol* 10:613. <https://doi.org/10.3389/FPHAR.2019.00613/BIBTEX>
- Bravo-Caparrós I, Ruiz-Cantero MC, Perazzoli G et al (2020) Sigma-1 receptors control neuropathic pain and macrophage infiltration into the dorsal root ganglion after peripheral nerve injury. *FASEB J* 34:5951–5966. <https://doi.org/10.1096/FJ.201901921R>
- Cendán CM, Pujalte JM, Portillo-Salido E et al (2005) Formalin-induced pain is reduced in sigma(1) receptor knockout mice. *Eur J Pharmacol* 511:73–74. <https://doi.org/10.1016/J.EJPHAR.2005.01.036>
- Chen H, Jiang L, Zhang D et al (2022) Exploring the correlation between the Regulation of Macrophages by Regulatory T Cells and Peripheral Neuropathic Pain. *Front Neurosci* 16. <https://doi.org/10.3389/FNINS.2022.813751>
- Cobos EJ, Nickerson CA, Gao F et al (2018) Mechanistic differences in Neuropathic Pain modalities revealed by correlating behavior with global expression profiling. *Cell Rep* 22:1301–1312. <https://doi.org/10.1016/J.CELREP.2018.01.006>
- Cortés-Montero E, Sánchez-Blázquez P, Onetti Y et al (2019) Ligands exert biased activity to regulate sigma 1 receptor interactions with cationic TRPA1, TRPV1, and TRPM8 channels. *Front Pharmacol* 10:634. <https://doi.org/10.3389/FPHAR.2019.00634/BIBTEX>
- Costigan M, Belfer I, Griffin RS et al (2010) Multiple chronic pain states are associated with a common amino acid-changing allele in KCNS1. *Brain* 133:2519–2527. <https://doi.org/10.1093/BRAIN/AWQ195>
- Davis-Taber RA, Scott VES (2006) Transcriptional profiling of dorsal root ganglia in a neuropathic pain model using microarray and laser capture microdissection. *Drug Dev Res* 67:308–330. <https://doi.org/10.1002/DDR.20096>
- de la Puente B, Nadal X, Portillo-Salido E et al (2009) Sigma-1 receptors regulate activity-induced spinal sensitization and neuropathic pain after peripheral nerve injury. *Pain* 145:294–303. <https://doi.org/10.1016/J.PAIN.2009.05.013>
- Decosterd I, Woolf CJ (2000) Spared nerve injury: an animal model of persistent peripheral neuropathic pain. *Pain* 87:149–158. [https://doi.org/10.1016/S0304-3959\(00\)00276-1](https://doi.org/10.1016/S0304-3959(00)00276-1)
- Denaro S, Pasquinucci L, Turnaturi R et al (2023) Sigma-1 receptor inhibition reduces mechanical Allodynia and modulate Neuroinflammation in Chronic Neuropathic Pain. <https://doi.org/10.1007/S12035-023-03717-W>. *Mol Neurobiol*
- Du X, Gamper N (2013) Potassium channels in peripheral pain pathways: expression, function and therapeutic potential. *Curr Neuropharmacol* 11:621–640. <https://doi.org/10.2174/1570159X113119990042>
- Entrena JM, Cobos EJ, Nieto FR et al (2009) Sigma-1 receptors are essential for capsaicin-induced mechanical hypersensitivity: studies with selective sigma-1 ligands and sigma-1 knockout mice. *Pain* 143:252–261. <https://doi.org/10.1016/J.PAIN.2009.03.011>
- Ewels P, Magnusson M, Lundin S, Käller M (2016) MultiQC: summarize analysis results for multiple tools and samples in a single report. *Bioinformatics* 32:3047–3048. <https://doi.org/10.1093/BIOINFORMATICS/BTW354>
- Frankish A, Diekhans M, Jungreis I et al (2021) GENCODE 2021. *Nucleic Acids Res* 49:D916–D923. <https://doi.org/10.1093/NAR/GKAA1087>
- Garvey L, Nelson M, Latch N et al (2012) CNS effects of a CCR5 inhibitor in HIV-infected subjects: a pharmacokinetic and cerebral metabolite study. *J Antimicrob Chemother* 67:206–212. <https://doi.org/10.1093/JAC/DKR427>
- Ge B, Li J, Wei Z et al (2017) Functional expression of CCL8 and its interaction with chemokine receptor CCR3. *BMC Immunol* 18. <https://doi.org/10.1186/S12865-017-0237-5>
- Ghazizaeidi S, Muley MM, Salter MW (2023) Neuropathic Pain: mechanisms, sex differences, and potential therapies for a global problem. *Annu Rev Pharmacol Toxicol* 63:565–583. <https://doi.org/10.1146/ANNUREV-PHARMTOX-051421-112259>
- Gu Z, Eils R, Schlesner M (2016) Complex heatmaps reveal patterns and correlations in multidimensional genomic data. *Bioinformatics* 32:2847–2849. <https://doi.org/10.1093/BIOINFORMATICS/BTW313>
- Gulick RM, Lalezari J, Goodrich J et al (2008) Maraviroc for previously treated patients with R5 HIV-1 infection. *N Engl J Med* 359:1429–1441. <https://doi.org/10.1056/NEJMOA0803152>
- Hall BE, Macdonald E, Cassidy M et al (2022) Transcriptomic analysis of human sensory neurons in painful diabetic neuropathy reveals inflammation and neuronal loss. *Scientific Reports* 2022 12:1 12:1–16. <https://doi.org/10.1038/s41598-022-08100-8>
- Halvorsen EC, Hamilton MJ, Young A et al (2016) Maraviroc decreases CCL8-mediated migration of CCR5(+) regulatory T cells and reduces metastatic tumor growth in the lungs. *Oncimmunology* 5:e1150398. <https://doi.org/10.1080/2162402X.2016.1150398>
- Horvath S, Zhang B, Carlson M et al (2006) Analysis of oncogenic signaling networks in glioblastoma identifies ASPM as a molecular target. *Proc Natl Acad Sci U S A* 103:17402–17407. <https://doi.org/10.1073/PNAS.0608396103>
- Ino Y, Maruyama M, Shimizu M et al (2023) TSLP in DRG neurons causes the development of neuropathic pain through T cells. *J Neuroinflammation* 20. <https://doi.org/10.1186/S12974-023-02882-Y>
- Ji RR, Xu ZZ, Gao YJ (2014) Emerging targets in neuroinflammation-driven chronic pain. *Nat Rev Drug Discov* 13:533–548. <https://doi.org/10.1038/NRD4334>
- Ji RR, Nackley A, Huh Y et al (2018) Neuroinflammation and Central Sensitization in chronic and widespread Pain. *Anesthesiology* 129:343–366. <https://doi.org/10.1097/ALN.0000000000002130>
- Kim D, Paggi JM, Park C et al (2019) Graph-based genome alignment and genotyping with HISAT2 and HISAT-genotype. *Nat Biotechnol* 37:907–915. <https://doi.org/10.1038/S41587-019-0201-4>
- Kwiatkowski K, Piotrowska A, Rojewska E et al (2016) Beneficial properties of maraviroc on neuropathic pain development and opioid effectiveness in rats. *Prog Neuropsychopharmacol Biol Psychiatry* 64:68–78. <https://doi.org/10.1016/J.PNPBP.2015.07.005>
- Lacroix-Fralish ML, Austin JS, Zheng FY et al (2011) Patterns of pain: meta-analysis of microarray studies of pain. *Pain* 152:1888–1898. <https://doi.org/10.1016/J.PAIN.2011.04.014>
- Laedermann CJ, Pertin M, Suter MR, Decosterd I (2014) Voltage-gated sodium channel expression in mouse DRG after SNI leads to re-evaluation of projections of injured fibers. *Mol Pain* 10:19. <https://doi.org/10.1186/1744-8069-10-19>
- Langfelder P, Horvath S (2008) WGCNA: an R package for weighted correlation network analysis. *BMC Bioinformatics* 9:559. <https://doi.org/10.1186/1471-2105-9-559>
- Li B, Dewey CN (2011) RSEM: accurate transcript quantification from RNA-Seq data with or without a reference genome. *BMC Bioinformatics* 12:323. <https://doi.org/10.1186/1471-2105-12-323>
- Lindborg JA, Niemi JP, Howarth MA et al (2018) Molecular and cellular identification of the immune response in peripheral ganglia following nerve injury. *J Neuroinflammation* 15:192. <https://doi.org/10.1186/S12974-018-1222-5>
- Love MI, Huber W, Anders S (2014) Moderated estimation of Fold change and dispersion for RNA-seq data with DESeq2. *Genome Biol* 15:550. <https://doi.org/10.1186/S13059-014-0550-8>

- Lu Y, Jiang BC, Cao DL et al (2017) Chemokine CCL8 and its receptor CCR5 in the spinal cord are involved in visceral pain induced by experimental colitis in mice. *Brain Res Bull* 135:170–178. <https://doi.org/10.1016/J.BRAINRESBULL.2017.10.009>
- Marcotti A, Fernández-Trillo J, González A et al (2023) TRPA1 modulation by Sigma-1 receptor prevents oxaliplatin-induced painful peripheral neuropathy. *Brain* 146:475–491. <https://doi.org/10.1093/BRAIN/AWAC273>
- Merlos M, Burgueño J, Portillo-Salido E et al (2017) Pharmacological modulation of the Sigma 1 receptor and the treatment of Pain. *Adv Exp Med Biol* 964:85–107. https://doi.org/10.1007/978-3-319-50174-1_8
- Mogil JS, Graham AC, Ritchie J et al (2010) Hypolocomotion, asymmetrically directed behaviors (licking, lifting, flinching, and shaking) and dynamic weight bearing (gait) changes are not measures of neuropathic pain in mice. *Mol Pain* 6:34. <https://doi.org/10.1186/1744-8069-6-34>
- Montilla-García Á, Perazzoli G, Tejada M et al (2018) Modality-specific peripheral antinociceptive effects of μ -opioid agonists on heat and mechanical stimuli: contribution of sigma-1 receptors. *Neuropharmacology* 135:328–342. <https://doi.org/10.1016/J.NEUROPHARM.2018.03.025>
- Moon JY, Roh DH, Yoon SY et al (2014) σ 1 receptors activate astrocytes via p38 MAPK phosphorylation leading to the development of mechanical allodynia in a mouse model of neuropathic pain. *Br J Pharmacol* 171:5881–5897. <https://doi.org/10.1111/BPH.12893>
- Moon JY, Choi SR, Roh DH et al (2015) Spinal sigma-1 receptor activation increases the production of D-serine in astrocytes which contributes to the development of mechanical allodynia in a mouse model of neuropathic pain. *Pharmacol Res* 100:353–364. <https://doi.org/10.1016/J.PHRS.2015.08.019>
- Nair A, Jacob S (2016) A simple practice guide for dose conversion between animals and human. *J Basic Clin Pharm* 7:27. <https://doi.org/10.4103/0976-0105.177703>
- Ochoa-Callejero L, Pérez-Martínez L, Rubio-Mediavilla S et al (2013) Maraviroc, a CCR5 antagonist, prevents development of hepatocellular carcinoma in a mouse model. *PLoS ONE* 8:e53992. <https://doi.org/10.1371/JOURNAL.PONE.0053992>
- Okonechnikov K, Conesa A, García-Alcalde F (2016) Qualimap 2: advanced multi-sample quality control for high-throughput sequencing data. *Bioinformatics* 32:292–294. <https://doi.org/10.1093/BIOINFORMATICS/BTV566>
- Pérez-Martínez L, Romero L, Muñoz-Galván S et al (2020) Implications of maraviroc and/or rapamycin in a mouse model of fragility. *Aging* 12:8565–8582. <https://doi.org/10.18632/AGING.103167>
- Piotrowska A, Kwiatkowski K, Rojewska E et al (2016) Maraviroc reduces neuropathic pain through polarization of microglia and astroglia - evidence from in vivo and in vitro studies. *Neuropharmacology* 108:207–219. <https://doi.org/10.1016/J.NEUROPHARM.2016.04.024>
- Rosario MC, Jacqmin P, Dorr Pet al (2008) Population pharmacokinetic/pharmacodynamic analysis of CCR5 receptor occupancy by maraviroc in healthy subjects and HIV-positive patients. *Br J Clin Pharmacol* 65:86. <https://doi.org/10.1111/J.1365-2125.2008.03140.X>
- Ruffing N, Sullivan N, Sharmeen L et al (1998) CCR5 has an expanded ligand-binding repertoire and is the primary receptor used by MCP-2 on activated T cells. *Cell Immunol* 189:160–168. <https://doi.org/10.1006/CIMM.1998.1379>
- Ruiz-Cantero MC, González-Cano R, Tejada M et al (2021) Sigma-1 receptor: a drug target for the modulation of neuroimmune and neuroglial interactions during chronic pain. *Pharmacol Res* 163:105339. <https://doi.org/10.1016/J.PHRS.2020.105339>
- Ruiz-Cantero MC, Cortés-Montero E, Jain A et al (2023a) The sigma-1 receptor curtails endogenous opioid analgesia during sensitization of TRPV1 nociceptors. *Br J Pharmacol* 180:1148–1167. <https://doi.org/10.1111/BPH.16003>
- Ruiz-Cantero MC, Huerta MÁ, Tejada MÁ et al (2023b) Sigma-1 receptor agonism exacerbates immune-driven nociception: role of TRPV1+nociceptors. *Biomed Pharmacother* 167:115534. <https://doi.org/10.1016/J.BIOPHA.2023.115534>
- Sánchez-Fernández C, Montilla-García Á, González-Cano R et al (2014) Modulation of peripheral μ -opioid analgesia by σ 1 receptors. *J Pharmacol Exp Ther* 348:32–45. <https://doi.org/10.1124/JPET.113.208272>
- Shin SM, Wang F, Qiu C et al (2022) Sigma-1 receptor activity in primary sensory neurons is a critical driver of neuropathic pain. *Gene Ther* 29:1–15. <https://doi.org/10.1038/S41434-020-0157-5>
- Sorge RE, Mapplebeck JCS, Rosen S et al (2015) Different immune cells mediate mechanical pain hypersensitivity in male and female mice. *Nat Neurosci* 18:1081–1083. <https://doi.org/10.1038/NN.4053>
- Stanford WL, Haque S, Alexander R et al (1997) Altered proliferative response by T lymphocytes of Ly-6A (Sca-1) null mice. *J Exp Med* 186:705. <https://doi.org/10.1084/JEM.186.5.705>
- Tarazona S, García-Alcalde F, Dopazo J et al (2011) Differential expression in RNA-seq: a matter of depth. *Genome Res* 21:2213–2223. <https://doi.org/10.1101/GR.124321.111>
- Tsai S-Y, Hayashi T, Mori T, Su T-P (2009) Sigma-1 receptor chaperones and diseases. *Cent Nerv Syst Agents Med Chem* 9:184–189. <https://doi.org/10.2174/1871524910909030184>
- Vicuña L, Strohlic DE, Latremoliere A et al (2015) The serine protease inhibitor SerpinA3N attenuates neuropathic pain by inhibiting T cell-derived leukocyte elastase. *Nat Med* 21:518–523. <https://doi.org/10.1038/NM.3852>
- Vidal-Torres A, de la Puente B, Rocasalbas M et al (2013) Sigma-1 receptor antagonism as opioid adjuvant strategy: enhancement of opioid antinociception without increasing adverse effects. *Eur J Pharmacol* 711:63–72. <https://doi.org/10.1016/J.EJPBAR.2013.04.018>
- Wong GT (2002) Speed congenics: applications for transgenic and knock-out mouse strains. *Neuropeptides* 36:230–236. <https://doi.org/10.1054/npep.2002.0905>
- Yokoyama H, Hirai T, Nagata T et al (2020) DNA microarray analysis of Differential Gene expression in the dorsal Root ganglia of four different neuropathic Pain Mouse models. *J Pain Res* 13:3031–3043. <https://doi.org/10.2147/JPR.S272952>
- Zheng Q, Xie W, Lückemeyer DD et al (2022) Synchronized cluster firing, a distinct form of sensory neuron activation, drives spontaneous pain. *Neuron* 110:209–220e6. <https://doi.org/10.1016/J.NEURON.2021.10.019>
- Zhu X, Cao S, Zhu M, Di et al (2014) Contribution of chemokine CCL2/CCR2 signaling in the dorsal root ganglion and spinal cord to the maintenance of neuropathic pain in a rat model of lumbar disc herniation. *J Pain* 15:516–526. <https://doi.org/10.1016/J.JPAIN.2014.01.492>

Publisher's Note Springer Nature remains neutral with regard to jurisdictional claims in published maps and institutional affiliations.

Springer Nature or its licensor (e.g. a society or other partner) holds exclusive rights to this article under a publishing agreement with the author(s) or other rightsholder(s); author self-archiving of the accepted manuscript version of this article is solely governed by the terms of such publishing agreement and applicable law.